

Hydraulic and Mechanical Properties Affecting Ground-Water Flow and Aquifer- System Compaction, San Joaquin Valley, California

By Michelle Sneed

U.S. GEOLOGICAL SURVEY

Open-File Report 01-35

Prepared in cooperation with the
U.S. BUREAU OF RECLAMATION

6441-23

Sacramento, California
2001

U.S. DEPARTMENT OF THE INTERIOR
GALE A. NORTON, Secretary

U.S. GEOLOGICAL SURVEY
Charles G. Groat, Director

The use of firm, trade, and brand names in this report is for identification purposes only and does not constitute endorsement by the U.S. Geological Survey.

For additional information write to:

District Chief
U.S. Geological Survey
Placer Hall, Suite 2012
6000 J Street
Sacramento, CA 95819-6129

Copies of this report can be purchased
from:

U.S. Geological Survey
Information Services
Box 25286
Federal Center
Denver, CO 80225

CONTENTS

Abstract.....	1
Introduction	1
Purpose and Scope.....	3
Location of Study Area.....	3
Hydrogeologic Setting.....	3
Aquifer-System Storage.....	4
Elastic and Inelastic Compressibility (Specific Storage).....	4
Aquifer-System Storage Coefficients	5
Estimates Of Aquifer-System Storage Values.....	5
Aquifer-Test Analyses	5
Stress-Strain Analyses of Borehole Extensometer Observations	7
Laboratory Consolidation Tests	11
Model Simulations.....	11
Evaluation of Specific-Storage Values.....	24
Summary.....	25
References	25

FIGURES

1. Location of selected features in the Central Valley, California	2
2. Relation of WESTSIM (U.S. Bureau of Reclamation) model domain and RASA (U.S. Geological Survey) model domain	18

TABLES

1. Storage coefficients estimated from results of aquifer tests near Pixley, California, February 1961 and March 1963	6
2. Aquifer-system properties estimated from results of stress-strain analyses of borehole extensometer observations, San Joaquin Valley, California	8
3. Consolidation test summaries	12
4. Aquifer-system properties estimated from results of calibrated models, San Joaquin Valley, California	16
5. Aquifer-system properties used in Regional Aquifer-System Analysis simulations.....	20

CONVERSION FACTORS, VERTICAL DATUM, ABBREVIATIONS, WELL-NUMBERING SYSTEM, AND SYMBOLS

Conversion Factors

	Multiply	By	To obtain
foot (ft)		0.3048	meter
foot per year (ft/yr)		0.3048	meter per year
gallon per minute (gal/min)		0.06308	liter per second
inch (in.)		25.4	millimeter
mile (mi)		1.609	kilometer
pound per square inch (lb/in ²)		6.895	kilopascal
square foot per year (ft ² /yr)		0.09290	square meter per year
square mile (mi ²)		2.590	square kilometer

Vertical Datum

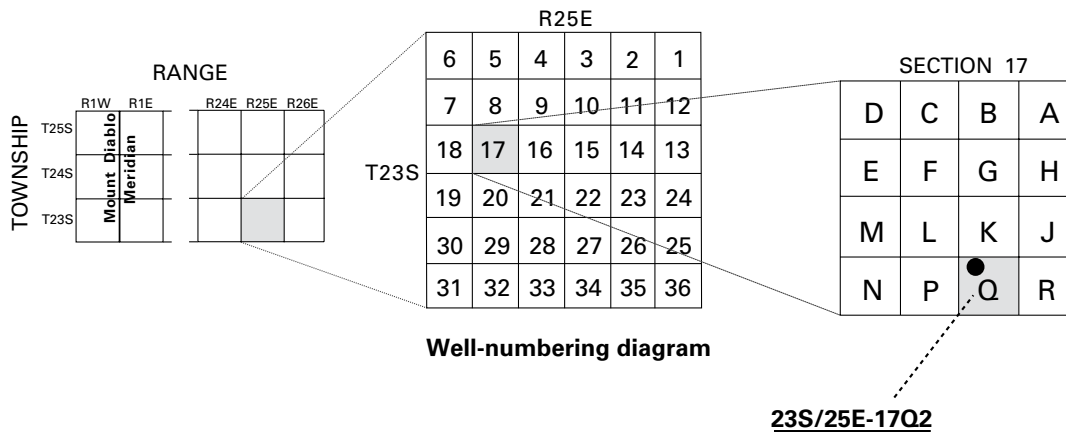
Sea level: In this report, "sea level" refers to the National Geodetic Vertical Datum of 1929 (NGVD of 1929)—a geodetic datum derived from a general adjustment of the first-order level nets of both the United States and Canada, formerly called Sea Level Datum of 1929.

Abbreviations

- USBR U.S. Bureau of Reclamation
- RASA Regional Aquifer-System Analysis

Well-Numbering System

Wells are identified and numbered according to their location in the rectangular system for the subdivision of public lands. Identification consists of the township number, north or south; the range number, east or west; and the section number. Each section is divided into sixteen 40-acre tracts lettered consecutively (except I and O), beginning with "A" in the northeast corner of the section and progressing in a sinusoidal manner to "R" in the southeast corner. Within the 40-acre tract, wells are sequentially numbered in the order they are inventoried. The final letter refers to the base line and meridian. In California, there are three base lines and meridians: Humboldt (H), Mount Diablo (M), and San Bernardino (S). All wells in the study area are referenced to the Mount Diablo base line and meridian (M). Well numbers consist of 15 characters and follow the format 023S025E17Q002M. In this report, well numbers are abbreviated and written 23S/25E-17Q2. Wells in the same township and range are referred to only by their section designation, -17Q2. The following diagram shows how the number for well 23S/25E-17Q2 is derived.



Symbols, in order of appearance

σ_e	effective or intergranular stress
p	pore-fluid pressure
Δ	change (for example, $\Delta\sigma_e$ means change in effective stress)
h	hydraulic head
ρ	fluid density
g	gravitational acceleration
S^*_{sk}	aquifer-system skeletal specific storage
α^*_k	aquifer-system skeletal compressibility
*	aquifer-system property
(k)	skeletal component of specific storage, compressibility, or storage coefficient
S'_{sk}	aquitard skeletal specific storage
S'_{ske}	aquitard elastic skeletal specific storage
α'_{ke}	aquitard elastic skeletal compressibility
<	less than
$\sigma_{e(max)}$	past maximum effective or intergranular stress
S'_{skv}	aquitard inelastic skeletal specific storage
α'_{kv}	aquitard inelastic skeletal compressibility
>	greater than
'	aquitard property
(e)	elastic property
(v)	inelastic property
S_{sk}	aquifer skeletal specific storage
S_{ske}	aquifer elastic skeletal specific storage
α_{ke}	aquifer elastic skeletal compressibility
$\Sigma b'$	aggregate thickness of aquitards
Σb	aggregate thickness of aquifers
S'_k	aquitard skeletal storage coefficient
S_k	aquifer skeletal storage coefficient
S'_{ke}	aquitard elastic skeletal storage coefficient
S'_{kv}	aquitard inelastic skeletal storage coefficient
S_{ke}	aquifer elastic skeletal storage coefficient
β_f	fluid compressibility of water
S_w	aquifer-system storage attributed to the pore water
S'_{sw}	specific storage of water of aquitards
S_{sw}	specific storage of water of aquifers
n'	porosity of the aquitards
n	porosity of the aquifers
S^*	aquifer-system storage coefficient
S^*_v	aquifer-system inelastic storage coefficient

\approx	approximately equal to
S_{ke}^*	aquifer-system elastic skeletal storage coefficient
S_{ske}^*	aquifer-system elastic skeletal specific storage
S_k^*	aquifer-system skeletal storage coefficient
S_{kv}^*	aquifer-system inelastic skeletal storage coefficient
S_{skv}^*	aquifer-system inelastic skeletal specific storage
c_v	coefficient of consolidation
K_v	vertical hydraulic conductivity
T_{50}	time factor at 50-percent consolidation
H_{50}	one-half specimen thickness at 50-percent consolidation
t_{50}	time required to reach 50-percent consolidation
γ_w	specific weight of water
e_o	initial void ratio
e	final void ratio
K'_v	aquitard vertical hydraulic conductivity
\hat{S}_{skv}	sample inelastic skeletal specific storage

Hydraulic and Mechanical Properties Affecting Ground-Water Flow and Aquifer-System Compaction, San Joaquin Valley, California

By Michelle Sneed

ABSTRACT

This report summarizes hydraulic and mechanical properties affecting ground-water flow and aquifer-system compaction in the San Joaquin Valley, a broad alluviated intermontane structural trough that constitutes the southern two-thirds of the Central Valley of California. These values will be used to constrain a coupled ground-water flow and aquifer-system compaction model of the western San Joaquin Valley called WESTSIM. A main objective of the WESTSIM model is to evaluate potential future land subsidence that might occur under conditions in which deliveries of imported surface water for agricultural use are reduced and ground-water pumping is increased. Storage values generally are components of the total aquifer-system storage and include inelastic and elastic skeletal storage values of the aquifers and the aquitards that primarily govern the potential amount of land subsidence. Vertical hydraulic conductivity values generally are for discrete thicknesses of sediments, usually aquitards, that primarily govern the rate of land subsidence. The data were compiled from published sources and include results of aquifer tests, stress-strain analyses of borehole extensometer observations, laboratory consolidation tests, and calibrated models of aquifer-system compaction.

INTRODUCTION

The San Joaquin Valley (fig. 1), a broad alluviated intermontane structural trough, constitutes the southern two-thirds of the Central Valley of California (Poland and others, 1975; Lofgren, 1976; Ireland, 1986). The Central Valley and pertinent features in the area of focus—the San Joaquin Valley—are shown on figure 1.

Land subsidence owing to ground-water withdrawal began in the San Joaquin Valley during the mid-1920s. By 1970, the maximum subsidence exceeded 28 ft (Poland and others, 1975) and reached 29.7 ft in 1981. More than 5,200 mi² of irrigable land, nearly one-half of the entire valley, has subsided at least 1 ft (Ireland, 1986). The subsidence occurred so slowly and uniformly over such a broad area throughout most of the affected area that its effects have been largely unnoticed by most observers. Locally, however, the differential subsidence has appeared abrupt and nonuniform, resulting in severe problems in the design and maintenance of canals and waterways, the expenditure of millions of dollars in repair and replacement of deep irrigation wells, and changes in irrigation and other farming practices (Lofgren, 1976).

The importation of surface water to subsiding areas by way of canals, such as the Friant–Kern and Delta–Mendota canals beginning in the 1950s, and the California Aqueduct beginning in 1968, reduced the pumping of ground water in these areas and reversed the rapid decline of hydraulic head (measured as water levels in wells) starting in the late 1960s and early 1970s. In 1983, ground-water levels in most actively subsiding areas of the San Joaquin Valley had returned

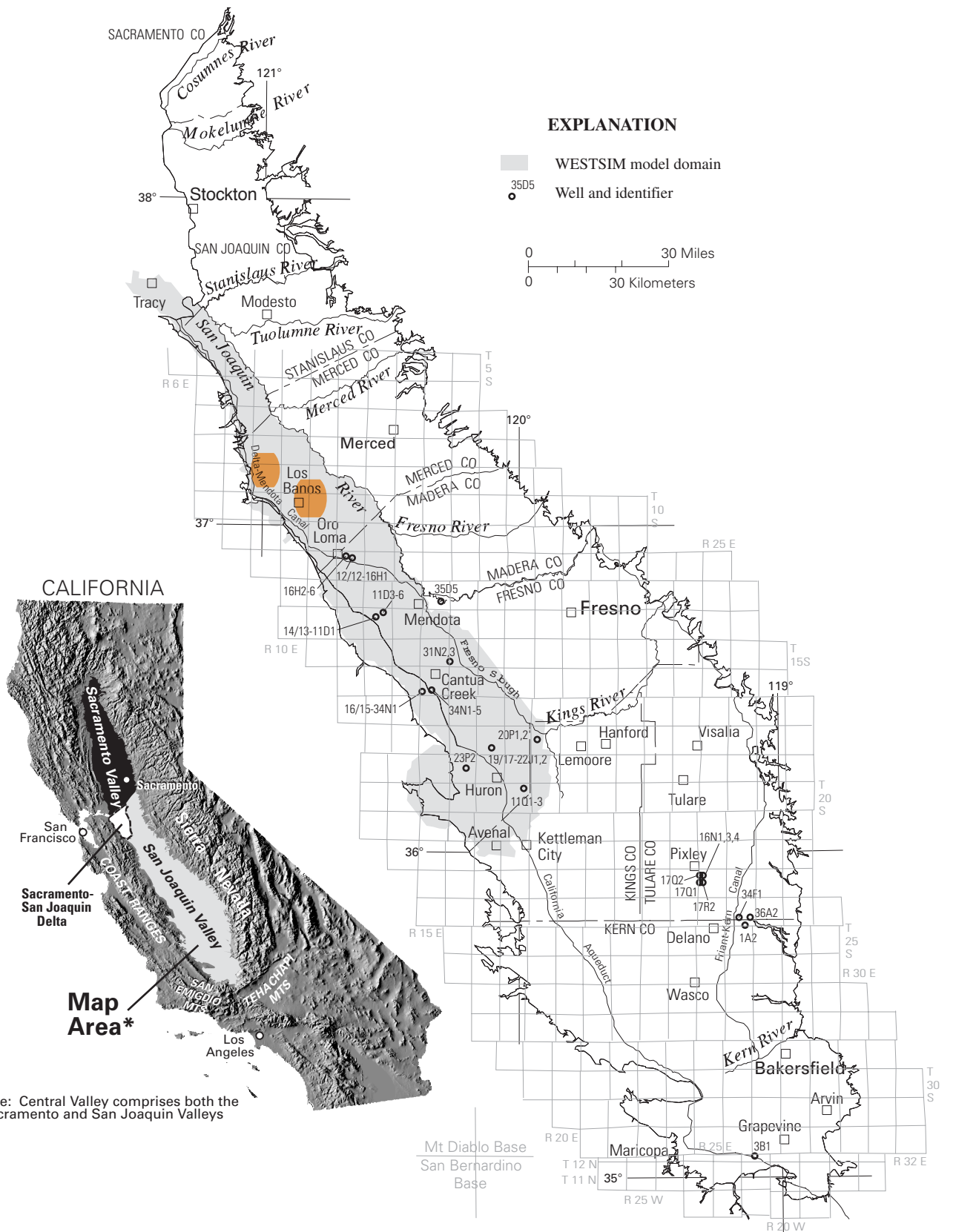


Figure 1. Location of selected features in the Central Valley, California.

to, or recovered above, their 1940–1950 levels, and the subsidence had slowed considerably or ceased (Ireland, 1986).

A detailed ground- and surface-water flow model of the western San Joaquin Valley called WESTSIM is being developed by the U.S. Bureau of Reclamation (USBR) to evaluate potential future land subsidence that might occur under conditions in which deliveries of imported surface water for agricultural use are reduced, resulting in increased ground-water pumping. A realistic model of land subsidence requires realistic values of model parameters that govern the magnitude and timing of aquifer-system compaction and the resulting land subsidence. These values include the skeletal specific storage, thickness, and vertical hydraulic conductivity of the aquitards. This report principally focusses on the skeletal specific storage values; vertical hydraulic conductivity of the aquitards is a secondary focus, and thicknesses of aquitards are minimally discussed.

Purpose and Scope

This report summarizes hydraulic and mechanical properties for the aquifer system in the San Joaquin Valley. The data were compiled from published sources and include results of aquifer tests, stress-strain analyses of borehole extensometer observations, laboratory consolidation tests, and calibrated models of aquifer-system compaction. These data will be used by the USBR to model ground-water flow and aquifer-system compaction (land subsidence) in a coupled ground-water flow and land subsidence model of the western San Joaquin Valley (WESTSIM).

Location of Study Area

The San Joaquin Valley includes roughly the southern two-thirds of the Central Valley of California (fig. 1). It is a broad structural trough surrounded on three sides by mountains—the Sierra Nevada on the east, the Coast Ranges on the west, and the Tehachapi and San Emigdio mountains on the south. The San Joaquin Valley is separated from the Sacramento Valley on the north by the combined deltas of the Sacramento and San Joaquin rivers. The valley extends 250 mi southward from north of Stockton to Grapevine at the foot of the Tehachapi Mountains. The width of the

valley floor ranges from 25 mi near Bakersfield to 55 mi near Visalia and averages about 35 mi. The area of the valley floor is 10,000 mi², excluding the rolling foothills that skirt the mountains (Davis and others, 1959; Poland and others, 1975; Lofgren, 1976; Ireland, 1986).

The geographic focus of this report, coincident with the WESTSIM model domain, is the western part of the San Joaquin Valley, which includes lands from Tracy on the north to Avenal on the south, and from the valley-side of the Coast Ranges on the west to the San Joaquin River and Fresno Slough on the east (fig. 1). Surrounding areas were included in this report, however, especially east of the WESTSIM model domain, because the estimates of hydraulic and mechanical properties in that area may be useful for comparable areas within the WESTSIM model domain.

Hydrogeologic Setting

The San Joaquin Valley is a major structural trough whose main axis trends northwest-southeast. Throughout Late Cretaceous (Mesozoic Era) and Tertiary (Cenozoic Era) Periods of geologic time, thousands of feet of shallow-water marine sediments were deposited in this down-warping geosyncline. Overlying these marine deposits are continental deposits of late Cenozoic age. In aggregate, these marine and continental deposits form an immense wedge that thickens from east to west and from north to south. At the extreme southern end of the valley, the thickness of sediments exceeds 28,000 ft (Lofgren, 1976).

The valley was formed chiefly by tectonic movement during late Cenozoic (late Tertiary Period and Quaternary Period) time that included major westward tilting of the Sierra Nevada block. Quaternary deformation has been principally along the southern and western borders of the valley, where the marine and continental rocks are tightly faulted and folded and the stream terraces are conspicuously elevated (Lofgren, 1976). A detailed discussion of the geology of the entire Central Valley is given by Page (1986).

Ground water in the San Joaquin Valley occurs under confined and unconfined conditions. Three distinct ground-water bodies exist in much of the western, central, and southeastern parts of the valley. In downward succession, these include (1) a body of unconfined and semiconfined fresh water in alluvial deposits overlying a widespread lacustrine confining bed—the

Corcoran Clay Member of the Tulare Formation (hereinafter called the Corcoran Clay), (2) an extensive reservoir of fresh water confined beneath the Corcoran Clay in alluvial and lacustrine deposits, and (3) a body of saline water contained in marine sediments that underlies the fresh water body throughout the area. In much of the eastern part of the valley, especially in the areas of major streams, the Corcoran Clay is not present and ground water occurs as one fresh water body to considerable depth (Lofgren, 1976).

AQUIFER-SYSTEM STORAGE

The concepts relating the compressibility of the aquifer system and its storage properties are briefly reviewed in the following sections. Various storage terms are used to define and delineate the components of the aquifer system that contribute to the total aquifer-system storage. The term “aquifer system” refers to a complex set of variably extensive, faulted, and interbedded aquifers (coarse-grained sediments) and aquitards (fine-grained sediments) that function regionally as a water-yielding unit (Poland and others, 1972). Correct application of the storage values in this report requires an understanding of these terms.

Elastic and Inelastic Compressibility (Specific Storage)

Under saturated confined conditions, the skeletal component of compressibility of an aquifer system governs the inverse change in volume and direct change in density of the material in response to a change in the intergranular stress. The law of effective stress (Terzaghi, 1925) states that when total stress on the aquifer system does not vary, the change in intergranular (effective) stress, σ_e , is related to the change in pore-fluid pressure, p , by

$$\Delta\sigma_e = -\Delta p$$

Fluid pressure variations cause equal but oppositely sensed changes in intergranular stress. Expressed in terms of hydraulic head, h :

$$h = p/\rho g$$

where ρ is the density of the pore water and g is the acceleration resulting from gravity. The changes in intergranular stress can be determined by measuring or simulating hydraulic-head variations

$$\Delta\sigma_e = -\Delta h\rho g$$

assuming ρ is constant.

For the purposes of this report, the skeletal specific storage of an aquifer system, S_{sk}^* , is expressed in terms of the skeletal compressibility, α_{sk}^* , where the subscript k refers to the skeletal component of specific storage or compressibility and the superscript $*$ refers to an aquifer-system property. Specific storage represents the volume of fluid taken into, or released from, a unit volume of aquifer-system sediment for a unit change in head (Lohman, 1972). The water being exchanged is derived from two processes—expansion or compression of the sediment that results from a change in effective stress, and expansion or compression of the fluid caused by a change in pore-fluid pressure.

The skeletal component of specific storage addresses the first of these processes, which for most unconsolidated alluvial aquifer systems is the dominant component. Skeletal compressibilities of fine-grained aquitards and coarser-grained aquifers typically differ by several orders of magnitude; therefore, it is useful to define them separately. Skeletal specific storages of the aquitards, S_{sk}' , are defined for two ranges of stress, elastic and inelastic.

$$S_{sk}' = \begin{cases} S_{ske}' = \alpha_{ke}'\rho g, & \sigma_e < \sigma_{e(max)} \\ S_{skv}' = \alpha_{kv}'\rho g, & \sigma_e > \sigma_{e(max)} \end{cases} \quad (1)$$

The primes (') signify aquitard properties, and the subscripts e and v refer to elastic and inelastic properties, respectively. For a change in effective stress, the aquitard deforms elastically when the effective stress remains less than the previous maximum effective stress, $\sigma_{e(max)}$; when the effective stress exceeds $\sigma_{e(max)}$, the aquitard deforms inelastically. For coarse-grained sediments typically found in aquifers, inelastic skeletal compressibility is negligible; therefore, skeletal specific storage of the aquifer, S_{sk} , is adequately represented by the fully recoverable, elastic component of skeletal specific storage, S_{ske} :

$$S_{sk} = S_{ske} = \alpha_{ke} \rho g \quad (2)$$

In typical aquifer systems consisting of unconsolidated to partly consolidated late Cenozoic sediments, inelastic specific storage generally is 20 to more than 100 times larger than elastic specific storage (Riley, 1998).

In the context of aquifer systems, the past maximum stress, or “preconsolidation stress,” can generally be represented by the previous lowest ground-water level. For stresses less than the preconsolidation stress—that is, ground-water levels higher than the preconsolidation-stress level—the aquifer system deforms (compresses or expands) elastically, and the deformation is recoverable. For stresses beyond the preconsolidation stress—ground-water levels lower than the preconsolidation-stress level—the pore structure of susceptible fine-grained sediment in the system may undergo significant rearrangement, resulting in a permanent (inelastic) reduction of pore volume and the vertical displacement of the land surface, or land subsidence.

Aquifer-System Storage Coefficients

The products of the elastic or inelastic skeletal specific storage values and the aggregate thickness of the aquitards, $\Sigma b'$, or aquifers, Σb , define the skeletal storage coefficients of the aquitards (S'_k) and the aquifers (S_k), respectively:

$$S'_k = \begin{cases} S'_{ke} = S'_{ske}(\Sigma b'), & \sigma_e < \sigma_{e(max)} \\ S'_{kv} = S'_{skv}(\Sigma b'), & \sigma_e > \sigma_{e(max)} \end{cases} \quad (3)$$

$$S_k = S_{ke} = S_{ske}(\Sigma b)$$

for the elastic (S'_{ke} and S_{ke}) and inelastic (S'_{kv}) ranges of skeletal compressibility. A separate equation relates the fluid compressibility of water, β_f to the component of aquifer-system storage attributed to the pore water, S_w :

$$S_w = S'_{sw}(\Sigma b') + S_{sw}(\Sigma b) = \beta_f \rho g [n'(\Sigma b') + n(\Sigma b)] \quad (4)$$

where n' and n are the porosities, and S'_{sw} and S_{sw} are the specific storages of water, of the aquitards and aquifers, respectively.

The aquifer-system storage coefficient, S^* , is defined as the sum of the skeletal storage coefficients of the aquitards and aquifers (eq. 3) plus the storage attributed to water compressibility (eq. 4).

$$S^* = S'_k + S_k + S_w \quad (5)$$

For compacting aquifer systems, S'_{kv} is much greater than S_w , and the inelastic storage coefficient of the aquifer system, S^*_v , is approximately equal to the aquitard inelastic skeletal storage coefficient.

$$S^*_v \approx S'_{kv} \quad (6)$$

In confined aquifer systems subjected to large-scale overdraft, the volume of water derived from irreversible aquitard compaction typically ranges from 10 to 30 percent of the total volume of ground water pumped (Riley, 1969). For some areas in the San Joaquin Valley, as much as 42 percent of the total volume of ground water pumped has been attributed to water derived from irreversible aquitard compaction (Prudic and Williamson, 1986).

ESTIMATES OF AQUIFER-SYSTEM STORAGE VALUES

The methods used by previous investigators to estimate storage and vertical hydraulic conductivity properties, and the results obtained, are discussed below. Four methods were used to estimate aquifer-system property values: aquifer-test analyses, stress-strain analyses of borehole extensometer observations, laboratory consolidation tests, and the results of calibrated model simulations.

Aquifer-Test Analyses

Aquifer-test analyses provide estimates of aquifer-system storage values using drawdown and recovery responses of water levels in wells to stresses, usually pumping-induced stresses from nearby wells. Aquifer tests generally provide information about

average properties for the coarse-grained sediment (aquifers) of the aquifer system (including the storage attributed to water compressibility, S_w), but not for the fine-grained sediment (aquitards). Storage values obtained using aquifer tests generally are constrained to the depth interval of the screen in the pumped well.

Riley and McClelland (1971) completed several aquifer tests at a site about 3 mi south of the town of Pixley (fig. 1). This site is known as the Pixley site and is within the Tulare–Wasco area of land subsidence (Lofgren and Klausning, 1969). The aquifer tests were done below the Corcoran Clay. The boundary of the eastern extent of the Corcoran Clay is 2.5 mi east of the Pixley site, and the clay extends at least 10 mi in all other directions. At the test site, the Corcoran Clay is 274 to 302 ft below land surface. Wells used in these tests are screened from 300 to 600 ft below land surface. The interval between 331 and 611 ft below land surface has 14 low-permeability beds ranging from 2 to 22 ft in thickness, totalling 178 ft, and 9 aquifers ranging from 8 to 22 ft in thickness, totalling 108 ft (Riley and McClelland, 1971).

The results of the aquifer tests were obtained during five episodes of drawdown and one of recovery, with two different wells pumping and four different rates of discharge in the five periods of pumping (table 1). At least one of two wells, 23S/25E-17Q2 and -17R2, was pumped during each of four tests done in February 1961 and March 1963; water levels were monitored in two or more wells, except for test 3 when water levels were monitored in a single well. The draw-down test of March 13–14, 1963 (test 4), produced the best suite of data (Riley and McClelland, 1971).

Results from the aquifer tests yielded storage coefficients for the aquifers that ranged between 2.4×10^{-5} and 1.6×10^{-4} ; if the largest and smallest values of the storage coefficient are discarded and the values estimated from the composite plot of test 1 are omitted, the values ranged from 2.8×10^{-5} to 7.2×10^{-5} (table 1). For a composite plot of data from the draw-down test of February 15–16, 1961 (test 1), the selected match points yielded storage coefficients of 2.5×10^{-5} for well 23S/25E-17R2 and 5.5×10^{-5} for wells 23S/25E-16N3 and -17Q1 (table 1). While pumping in 23S/25E-17R2 continued from test 4, well -17Q2 also

Table 1. Storage coefficients estimated from results of aquifer tests near Pixley, California, February 1961 and March 1963

[Table is modified from Riley and McClelland (1971). State well No.: See Well-Numbering System on p. IV. See figure 1 for location of wells. Test 1: well 23S/25E-17Q2 was pumped at 1,150 gallons per minute. Test 2: well 23S/25E-17Q2 was shut down. Test 3: wells 23S/25E-17Q2 and -17R2 were pumped at 1,150 and 825 gallons per minute, respectively. Test 4: well 23S/25E-17R2 was pumped at 750 gallons per minute. Test 5: well 23S/25E-17Q2 was pumped at 1,025 gallons per minute while pumping continued in well 23S/25E-17R2. —, not reported]

Observed well	Storage coefficient					Average by well ⁴
	Test 1 (Drawdown February 15–16, 1961)	Test 2 (Recovery February 16–17, 1961)	Test 3 (Drawdown February 17–20, 1961)	Test 4 (Drawdown March 13–14, 1963)	Test 5 (Drawdown March 14–16, 1963)	
23S/25E-16N3	¹ 5.3×10^{-5} ² 5.5×10^{-5}	7.2×10^{-5}	¹ 5.2×10^{-5} ³ 2.8×10^{-5}	5.6×10^{-5}	5.8×10^{-5}	5.3×10^{-5}
-17Q1	2.8×10^{-5} ² 5.5×10^{-5}	—	—	5.0×10^{-5}	1.6×10^{-4}	7.9×10^{-5}
-17Q2	—	—	—	3.4×10^{-5}	—	3.4×10^{-5}
-17R2	2.4×10^{-5} ² 2.5×10^{-5}	2.8×10^{-5}	—	—	4.9×10^{-5}	3.4×10^{-5}
Average by test ⁴	3.5×10^{-5}	5.0×10^{-5}	4.0×10^{-5}	4.7×10^{-5}	8.9×10^{-5}	
Average for all tests ⁴						5.2×10^{-5}
Average for all wells ⁴						5.0×10^{-5}

¹Value estimated from pumping well 23S/25E-17R2.

²Value estimated from selected match point on composite plot.

³Value estimated from pumping well 23S/25E-17Q2; value obtained from departure plot.

⁴Value excludes estimates made from composite plots.

was pumped for test 5 (March 14–16, 1963). Water-level responses in wells -16N3, -17Q1, and -17R2 to the two pumping wells were examined. The data were derived by plotting the departures from the drawdown trends established by the discharge of 23S/25E-17R2 and are subject to the inevitable inaccuracies of this process. The selected average match point yielded an approximate storage coefficient of 5.5×10^{-5} (Riley and McClelland, 1971).

Riley and McClelland (1971) concluded that the storage coefficient of the 300- to 600-ft confined, leaky aquifer system at the Pixley site is about 5×10^{-5} . From evidence on lithologic and geophysical logs, the maximum aquifer thickness to which the aggregate storage coefficient might apply would be about 100 ft. However, on the basis of the development of the cone of depression that is dominated by the flow and resulting head distribution in the most permeable and nearly continuous aquifers, it was estimated that the storage coefficient is applicable to 50 to 75 ft of aquifer thickness. On this basis, the average specific storage of the aquifer is about 7×10^{-7} to 1×10^{-6} ft⁻¹ (Riley and McClelland, 1971).

McClelland (1962; unpub. data, 1963, 1964) compiled data and results from aquifer tests done in the San Joaquin Valley prior to 1964, including the tests at the Pixley site. Because McClelland evaluated the quality of most tests as fair or poor, however, the storage properties that were derived are probably unreliable and are not reported here.

Poland (1961) generalized results from aquifer tests done in the Los Banos–Kettleman City area to demonstrate a drawback of using short-term aquifer tests when determining aquifer-system storage properties. The average value of 1×10^{-3} (derived from a short-term aquifer test) for the storage coefficient of a 700-ft thick aquifer was compared with a computed storage coefficient (5×10^{-2}) derived from compaction of the clayey sediments in this 700-ft interval on the basis of the ratio of subsidence to head decline. Poland (1961) concluded that storage derived from the short-term pumping test resulted in a volume about one-fiftieth of the long-term (15 to 25 years) yield from storage, but noted that this was an extreme example because the aquifer system is extremely compressible. Moreover, the amount of water derived from inelastic compression of the aquitards is variable. The amount of stored water yielded by the aquitards would be large only during the first decline of artesian pressure

(Poland, 1961). Prudic and Williamson (1986) used the ratio of the volume of water released from compaction and pumpage for the lower-pumped zone to estimate that from 35 to 42 percent of the water pumped comes from inelastic compaction.

Stress-Strain Analyses of Borehole Extensometer Observations

Elastic and inelastic skeletal storage coefficients have been estimated using a graphical method established by Riley (1969) using data from the Pixley site (23S/25E-16N) (fig. 1 and table 2). Riley's (1969) method is similar to the approach taken to determine the coefficients of compressibility from the stress-strain relations derived from laboratory consolidation tests. (Laboratory consolidation tests are discussed briefly in the following section). The method involves plotting applied stress (hydraulic head) on the *y*-axis versus either vertical strain or displacement (compaction) on the *x*-axis. Riley (1969) showed that for aquifer systems where pressure equilibration can occur rapidly between aquifers and aquitards, the inverse slopes measured from the predominant linear trends in the compaction-head trajectories represent measures of the skeletal storage coefficients. The elastic and inelastic components are limited to parts of the aquifer system that equilibrate relatively quickly to stress changes; results are not intended to be representative of thick aquitards, which typically equilibrate slowly.

For the Pixley site, Riley (1969) calculated that the aquifer-system elastic skeletal storage coefficient (S^*_{ke}) was about 1.1×10^{-3} and that the aquifer-system elastic skeletal specific storage (S^*_{ske}), corresponding to 405 ft of undifferentiated sediment in the depth interval 355–760 ft below land surface, was about 2.8×10^{-6} ft⁻¹ (table 2). Similarly, Riley (1969) calculated that the average skeletal storage coefficient of the aquifer system (S^*_k) was about 5.7×10^{-2} and that the corresponding average skeletal specific storage of the aquifer system, corresponding to 405 ft of undifferentiated sediment, was about 1.4×10^{-4} ft⁻¹ and ranged from about 1.1×10^{-4} to 1.8×10^{-4} ft⁻¹. Riley (1969) computed an average aquitard inelastic skeletal specific storage value of about 2.3×10^{-4} ft⁻¹ by dividing the aquifer-system skeletal storage coefficient by the aggregate thickness of compacting aquitards (table 2).

Table 2. Aquifer-system properties estimated from results of stress-strain analyses of borehole extensometer observations, San Joaquin Valley, California

[State well No.: See Well-Numbering System on p. IV. See figure 1 for location of wells. S^*_{sk} , aquifer-system skeletal storage coefficient; S^*_{sk} , aquifer-system skeletal specific storage; S^*_{ke} , aquifer-system elastic skeletal storage coefficient; S^*_{ske} , aquifer-system elastic skeletal specific storage; S^*_{kv} , aquifer-system inelastic skeletal storage coefficient; S^*_{skv} , aquifer-system inelastic skeletal specific storage; S'_{kv} , aquitard inelastic skeletal storage coefficient; S'_{skv} , aquitard inelastic skeletal specific storage; S_{ske} , aquifer elastic skeletal specific storage; K'_v , aquitard vertical hydraulic conductivity; ft, foot; ftbls, feet below land surface; ft^{-1} , per foot; ft/yr, foot per year; —, not reported; <, less than]

State well No.	Aggregate aquitard thickness (ft)	Combined thickness of the aquitard and aquifer (ft)	Interval of sediments (ftbls)	S^*_{sk}	S^*_{sk} (ft^{-1})	S^*_{ke}	S^*_{ske} (ft^{-1})	S^*_{kv}	S^*_{skv} (ft^{-1})	S'_{kv}	S'_{skv} (ft^{-1})	S_{ske} (ft^{-1})	K'_v (ft/yr)
⁶ 23S/25E-16N	246	405	355–760	5.7×10^{-2}	1.4×10^{-4}	1.1×10^{-3}	2.8×10^{-6}	—	—	—	2.3×10^{-4}	—	3.0×10^{-3}
(⁷)	—	330	430–760	—	—	—	1.9×10^{-6}	—	—	—	1.4×10^{-4}	—	—
(⁸)	230	330	430–760	—	—	6.4×10^{-4}	1.9×10^{-6}	6.8×10^{-2}	2.1×10^{-4}	1.68×10^{-2}	3.0×10^{-4}	—	—
(⁹)	—	330	430–760	—	—	6.4×10^{-4}	1.9×10^{-6}	—	—	—	—	—	—
(⁹)	—	100	330–430	—	—	7×10^{-4}	7.0×10^{-6}	—	—	—	—	—	—
(⁹)	—	430	330–760	—	—	1.3×10^{-3}	2.3×10^{-6}	—	—	—	—	—	—
^{8,9} 18S/19E-20P2	—	347	230–577	—	—	1.2×10^{-3}	3.4×10^{-6}	—	—	—	—	—	—
(¹⁰)	44	347	230–577	—	—	1.2×10^{-3}	3.5×10^{-6}	—	—	—	—	—	—
(¹⁰)	44	347	230–577	—	—	—	4.6×10^{-7}	—	—	—	—	—	—
(¹⁰)	44	347	230–577	—	—	—	3.6×10^{-6}	—	—	—	—	—	—
⁹ 15S/16E-31N3	—	276	320–596	—	—	1.06×10^{-3}	3.8×10^{-6}	—	—	—	—	—	—
⁹ 24S/26E-34F1	—	1,310	0–1,310	—	—	2.5×10^{-3}	1.9×10^{-6}	—	—	—	—	—	—
⁹ 25S/26E-1A2	—	892	0–892	—	—	6×10^{-4}	2.7×10^{-7}	—	—	—	—	—	—
¹⁰ 13S/15E-35D5	—	340	100–440	—	—	—	3.4×10^{-6}	—	—	—	—	—	—
(¹⁰)	—	340	100–440	—	—	—	4.0×10^{-6}	—	—	—	—	—	—

See footnotes at end of table.

Table 2. Aquifer-system properties estimated from results of stress-strain analyses of borehole extensometer observations, San Joaquin Valley, California—Continued

State well No.	Aggregate aquitard thickness (ft)	Combined thickness of the aquitard and aquifer (ft)	Interval of sediments (ftbls)	S^*_{k}	S^*_{sk} (ft ⁻¹)	S^*_{ke}	S^*_{ske} (ft ⁻¹)	S^*_{kv}	S^*_{skv} (ft ⁻¹)	S'_{kv}	S'_{skv} (ft ⁻¹)	S_{ske} (ft ⁻¹)	K'_v (ft/yr)
¹⁰ 19S/16E-23P2	—	<2,200	0–2,200	—	—	—	⁴ 7×10^{-7}	—	—	—	—	—	—
(¹⁰)	—	<2,200	0–2,200	—	—	—	⁵ 3.1×10^{-6}	—	—	—	—	—	—
(¹⁰)	—	<2,200	0–2,200	—	—	—	³ 1.4×10^{-6}	—	—	—	—	—	—
¹⁰ 14S/13E-11D6	758	<1,358	0–1,358	—	—	—	—	—	—	—	—	⁴ 1.6×10^{-6}	—
(¹⁰)	758	<1,358	0–1,358	—	—	—	—	—	—	—	—	⁵ 5.0×10^{-6}	—
(¹⁰)	758	<1,358	0–1,358	—	—	—	—	—	—	—	—	³ 3.3×10^{-6}	—

¹Assumes S'_{kv} equals S^*_{kv} .

²Calculated by dividing S^*_{ke} by combined thickness.

³Mean value of range.

⁴Smallest value in range.

⁵Largest value in range.

⁶Riley, 1969

⁷Lofgren, 1979

⁸Johnson, 1984

⁹Poland and others, 1975

¹⁰Bull and Poland, 1975

Lofgren (1979) expanded the interpretations of stress-strain plots from Pixley by focusing on a smaller thickness of sediments (330 ft in the depth interval 430–760 ft below land surface) and contrasting storage values obtained for each year of data to average values for the period of record. Lofgren (1979) computed a S^*_{ske} value of about $1.9 \times 10^{-6} \text{ ft}^{-1}$ and an aquitard inelastic skeletal specific-storage value of about $1.4 \times 10^{-4} \text{ ft}^{-1}$ (table 2) using the same method described above for Riley (1969). Lofgren concluded that the inelastic storage value approached the elastic value in 1962, 1963, and 1969, indicating that stresses did not exceed the preconsolidation stress during those years.

Johnson (1984) reported storage values for two sites: the Pixley site and well 18S/19E-20P2 near Lemoore (table 2). Johnson (1984) reported an aquifer-system elastic skeletal storage coefficient (S^*_{ke}) for the Pixley site of about 6.4×10^{-4} and a corresponding elastic skeletal specific storage (S^*_{ske}) (for about 330 ft of sediment in the depth interval 430–760 ft below land surface) of about $1.9 \times 10^{-6} \text{ ft}^{-1}$. The aquifer-system inelastic skeletal storage coefficient (S^*_{kv}) computed was about 6.8×10^{-2} , and the inelastic skeletal specific storage for the aquifer system (S^*_{skv}) was about $2.1 \times 10^{-4} \text{ ft}^{-1}$.

Johnson (1984) concluded that only the clay interbeds deform inelastically; hence the assumption was made that the S^*_{kv} equaled the inelastic skeletal storage coefficient of the aquitards. To obtain the average inelastic skeletal specific storage of the aquitards, $3.0 \times 10^{-4} \text{ ft}^{-1}$, the S^*_{kv} was divided by the aggregate thickness of aquitards (about 230 ft). For well 18S/19E-20P2, the depth interval measured is about 230–577 ft below land surface, the elastic skeletal storage coefficient of the aquifer system is about 1.2×10^{-3} , and the corresponding elastic skeletal specific storage is about $3.4 \times 10^{-6} \text{ ft}^{-1}$ (table 2) (Poland and others, 1975; Johnson, 1984).

Poland and others (1975) reported on storage values derived from stress-strain relations at five borehole extensometer sites in the San Joaquin Valley (table 2). Among these sites, Pixley (23S/25E-16N) was analyzed in detail by separating the aquifer system into two parts and analyzing the combined thickness; this was done using the multi-depth instrumentation. For the five sites, aquifer-system elastic skeletal storage coefficients ranged from about 6×10^{-4} to 2.5×10^{-3} (table 2). The corresponding aquifer-system elastic

skeletal specific storages ranged from about 6.7×10^{-7} to $7.0 \times 10^{-6} \text{ ft}^{-1}$. Inelastic storage values were not reported.

Bull and Poland (1975) reported elastic storage values for four sites (table 2). For well 18S/19E-20P2 in the depth interval 230–577 ft below land surface, the mean elastic skeletal storage coefficient reported was about 1.2×10^{-3} , corresponding to an aquifer-system elastic skeletal specific storage of about $3.5 \times 10^{-6} \text{ ft}^{-1}$, and ranged from about 6×10^{-7} to $3.6 \times 10^{-7} \text{ ft}^{-1}$.

For well site 13S/15E-35D5 in the depth interval 100–440 ft below land surface, Bull and Poland (1975) reported that the aquifer-system elastic skeletal specific storage ranged from about 3.4×10^{-6} to $4.0 \times 10^{-6} \text{ ft}^{-1}$.

For well site 19S/16E-23P2 in the depth interval 0–2,200 ft below land surface, the aquifer-system elastic skeletal specific storage ranged from about 7×10^{-7} to $3.1 \times 10^{-6} \text{ ft}^{-1}$ with a mean of about $1.4 \times 10^{-6} \text{ ft}^{-1}$. Bull and Poland (1975) reported that the most representative value may be larger than the mean.

For well site 14S/13E-11D6 in the depth interval 0–1,358 ft below land surface, Bull and Poland (1975) computed values representing coarser grained sediment (aquifers) by estimating the elastic changes for those deposits assumed to be sufficiently permeable to have little or no time delay for thickness changes during times of applied-stress (water-level) change. These coarser grained deposits undergoing elastic changes consist chiefly of sands, silts, and thinly-bedded clayey sands (Bull and Poland, 1975). A total of 118 ft of clayey sediments was not included in the computation of elastic change in thickness because of the time needed to expel water from aquitards upon increase in applied stress. The core record indicated that 540 ft of sandy deposits are present in the 658-ft interval between the base of the Corcoran Clay at a depth of 700 ft and the anchor depth (1,358 ft) of the compaction recorder (Bull and Poland, 1975). An additional 60 ft of sand is in the upper zone that is assumed to be compacting, and thus the aggregate thickness of the coarser grained deposits is about 600 ft. Bull and Poland (1975) reported that elastic skeletal specific storages of the coarser grained sediment ranged from about 1.6×10^{-6} to $5.0 \times 10^{-6} \text{ ft}^{-1}$ with a mean of about $3.3 \times 10^{-6} \text{ ft}^{-1}$.

Laboratory Consolidation Tests

Laboratory consolidation tests provide measurements of the coefficient of consolidation (in the inelastic range) and estimations of vertical hydraulic conductivity. The inelastic skeletal specific storage of the sample can be estimated by computing the ratio of the vertical hydraulic conductivity to the coefficient of consolidation (Jorgensen, 1980).

When a saturated soil sample is subjected to a load, that load initially is carried by the water in the voids of the sample because the water is relatively incompressible compared to the soil structure. If water can escape from the sample voids as a load is continually applied to the sample, an adjustment takes place wherein the load is gradually shifted to the soil structure. The process of load transference is generally slow for clay and is accompanied by a change in volume of the soil mass. Consolidation is defined as that gradual process that involves simultaneously a slow escape of water, a gradual compression, and a gradual pressure adjustment (Johnson and others, 1968). The theory of consolidation is discussed in detail by Terzaghi (1943).

To determine the rate and magnitude of consolidation of sediments, a small-scale laboratory test known as a one-dimensional consolidation test is used. The test and apparatus are described in detail by the U.S. Bureau of Reclamation (1974). The coefficient of consolidation, c_v , and vertical hydraulic conductivity, K_v , are computed from consolidation test results. The c_v represents the rate of consolidation for a given load increment. It is determined by use of the 50-percent point on the time-consolidation curve

$$c_v = (T_{50}H_{50}^2)/t_{50} \quad (7)$$

where T_{50} is a time factor at 50-percent consolidation, H_{50} is one-half the specimen thickness at 50-percent consolidation, and t_{50} is the time required for the specimen to reach 50-percent consolidation (Johnson, 1984). When the consolidation is complete under maximum loading, the consolidometer can be used as a variable-head permeameter, and the vertical hydraulic conductivity (K_v) of the soil sample can be determined directly

$$K_v = c_v(\gamma_w)(e_o - e)/\Delta p(1 + e_o) \quad (8)$$

where γ_w is the specific weight of water, e_o is the void ratio at start of load increment, e is the final void ratio, and Δp is the increment of load (Johnson and others, 1968). Once c_v and K_v are determined, the inelastic skeletal specific storage of the sample is computed by (Jorgensen, 1980)

$$\hat{S}_{skv} = K_v/c_v \quad (9)$$

Results of consolidation tests done on multiple samples in each of six coreholes in the San Joaquin Valley are given in table 3. Included are the core sample number; the depth interval where the sample was collected; the percentages of gravel, sand, and silt and clay for the sample; the load range applied to the sample; the coefficient of consolidation; the vertical hydraulic conductivity; and the inelastic skeletal specific storage. Additionally, the depth interval of the Corcoran Clay in each corehole is noted.

Model Simulations

Results from model simulations incorporate information about aquifer-system storage and hydraulic conductivity values. Models that simulate aquifer-system compaction generally include information about both the elastic and inelastic components of skeletal storage, and the vertical hydraulic conductivity. Model calibration can result in optimum estimates of the storage coefficients and the vertical hydraulic conductivity.

Helm (1975, 1976, 1977, 1978) inverse modeled several extensometer sites in the San Joaquin Valley, including the Pixley site, using a variety of methods; results were published in several papers (table 4). Helm (1975, 1976, 1977) simulated aggregate one-dimensional compaction of the series of aquitards at the Pixley site through use of a finite-difference representation of the vertical stress distribution within an idealized aquitard. This model simulated compaction at the Pixley site using constant parameters (Helm, 1975, 1977) and stress-dependent parameters (Helm, 1976). Helm (1975, 1976, 1977) used skeletal specific-storage values of aquitards derived from skeletal storage coefficients determined by Riley (1969) using the stress-strain graphical method. Repeat analysis of geophysical logs and micrologs changed Riley's estimate of total aquitard thickness within the total compacting

Table 3. Consolidation test summaries

[Table modified from table 9 in Johnson and others (1968). See figure 1 for location of coreholes (wells). Inelastic skeletal specific storage was calculated using equation 57 from Jorgensen (1980) (equation 9 in report). Contribution of water elasticity to specific storage was ignored. Name of nearest town to corehole in parentheses following corehole number. Depth interval of the Corcoran Clay Member of the Tulare Formation from plate 1 in Johnson and others (1968). >, more than; <, less than; c_v , coefficient of consolidation; K_v , vertical hydraulic conductivity; S_{sk}^{\wedge} , sample inelastic skeletal specific storage; ftbls, feet below land surface; mm, millimeter; lb/in², pound per square inch; ft²/yr, square foot per year; ft/yr, foot per year; ft⁻¹, per foot; —, no data]

Core sample No.	Depth interval (ftbls)	Gravel >4.76 mm (percent)	Sand, 4.76–0.074 mm (percent)	Silt and clay <0.074mm (percent)	Load range (lb/in ²)	c_v (ft ² /yr)	K_v (ft/yr)	S_{sk}^{\wedge} (ft ⁻¹)
Corehole 12S/12E-16H1 (Oro Loma)								
Corcoran Clay Member: 379–465 ftbls								
23L91	84.3–84.6	0	10	90	100–200	72.5	8.5×10^{-3}	1.2×10^{-4}
					200–400	31.8	2.0×10^{-3}	6.3×10^{-5}
92	159.4–159.8	0	10	90	100–200	20.1	2.8×10^{-3}	1.4×10^{-4}
					200–400	11.2	1.3×10^{-3}	1.2×10^{-4}
93	230.8–231.2	0	10	90	200–400	37.2	4.0×10^{-3}	1.1×10^{-4}
95	374.0–374.5	0	0	100	200–400	3.3	2.9×10^{-4}	8.8×10^{-5}
					400–800	2.2	1.5×10^{-4}	6.8×10^{-5}
96	425.0–425.3	0	10	90	200–400	0.92	3.2×10^{-4}	3.5×10^{-4}
					400–800	0.7	1.2×10^{-4}	1.7×10^{-4}
97	471.2–471.5	0	5	95	200–400	28.5	8.0×10^{-3}	2.8×10^{-4}
					400–800	28.5	3.6×10^{-3}	1.3×10^{-4}
99	579.0–579.3	0	35	65	200–400	122.0	7.2×10^{-3}	5.9×10^{-5}
					400–800	83.2	4.4×10^{-3}	5.3×10^{-5}
					800–1,600	54.8	1.5×10^{-3}	2.7×10^{-5}
100	625.0–625.4	0	0	100	400–800	3.7	2.6×10^{-4}	7.0×10^{-5}
					800–1,600	1.8	6.0×10^{-5}	3.3×10^{-5}
101	675.9–676.2	0	45	55	400–800	232.1	1.2×10^{-2}	5.2×10^{-5}
					800–1,600	151.1	4.8×10^{-3}	3.2×10^{-5}
102	722.0–722.3	0	5	95	400–800	5.9	3.3×10^{-4}	5.6×10^{-5}
					800–1,600	1.3	5.0×10^{-5}	3.8×10^{-5}
103	773.0–773.4	0	60	40	800–1,600	9.4	3.5×10^{-4}	3.7×10^{-5}
106	926.8–927.2	0	20	80	400–800	35.0	3.7×10^{-3}	1.1×10^{-4}
					800–1,600	18.6	1.2×10^{-3}	6.4×10^{-5}
Corehole 14S/13E-11D1 (Mendota)								
Corcoran Clay Member: 625–700 ftbls								
23L194	397.0–397.3	0	10	90	200–400	39.4	4.0×10^{-3}	1.0×10^{-4}
					400–800	11.2	8.1×10^{-4}	7.2×10^{-5}
					800–1,600	2.6	9.0×10^{-5}	3.5×10^{-5}
81	554.0–554.4	0	10	90	200–400	15.0	9.5×10^{-4}	6.3×10^{-5}
					400–800	4.9	2.2×10^{-4}	4.5×10^{-5}
					800–1,600	9.0	1.8×10^{-4}	2.0×10^{-5}
83	699.0–699.4	0	10	90	400–800	12.8	2.1×10^{-3}	1.6×10^{-4}
					800–1,600	7.1	5.0×10^{-4}	7.0×10^{-5}
84	746.0–746.4	0	45	55	200–400	37.4	2.6×10^{-3}	7.0×10^{-5}
					400–800	26.9	1.5×10^{-3}	5.6×10^{-5}
					800–1,600	14.5	5.5×10^{-4}	3.8×10^{-5}
196	832.2–832.7	0	60	40	200–400	43.8	3.6×10^{-3}	8.2×10^{-5}
					400–800	14.7	9.4×10^{-4}	6.4×10^{-5}
					800–1,600	9.9	3.7×10^{-4}	3.7×10^{-5}

Table 3. Consolidation test summaries—Continued

Core sample No.	Depth interval (ftbls)	Gravel >4.76 mm (percent)	Sand, 4.76–0.074 mm (percent)	Silt and clay <0.074mm (percent)	Load range (lb/in ²)	c _v (ft ² /yr)	K _v (ft/yr)	S [^] _{skv} (ft ⁻¹)
Corehole 14S/13E-11D1 (Mendota)								
Corcoran Clay Member: 625–700 ftbls—Continued								
85	983.6–984.0	0	5	95	200–400	2.6	2.1×10 ⁻⁴	8.1×10 ⁻⁵
					400–800	2.2	1.1×10 ⁻⁴	5.0×10 ⁻⁵
					800–1,600	2.6	1.2×10 ⁻⁴	4.6×10 ⁻⁵
89	1,395.0–1,395.3	0	0	100	200–400	21.8	1.2×10 ⁻³	5.5×10 ⁻⁵
					400–800	3.6	1.5×10 ⁻⁴	4.2×10 ⁻⁵
					800–1,600	2.4	8.0×10 ⁻⁵	3.3×10 ⁻⁵
90	1,450.0–1,450.3	0	45	55	800–1,600	8.4	2.4×10 ⁻⁴	2.9×10 ⁻⁵
Corehole 16S/15E-34N1 (Cantua Creek)								
Corcoran Clay Member: 565–575 ftbls								
23L197	299.1–299.5	0	0	100	200–400	74.9	1.1×10 ⁻²	1.5×10 ⁻⁴
198	418.1–418.5	0	0	100	100–200	361.4	6.3×10 ⁻²	1.7×10 ⁻⁴
					200–400	109.5	1.3×10 ⁻²	1.2×10 ⁻⁴
					400–800	30.7	2.1×10 ⁻³	6.8×10 ⁻⁵
200	538.9–539.2	0	0	100	200–400	74.5	6.3×10 ⁻³	8.5×10 ⁻⁵
					400–800	28.5	2.1×10 ⁻³	7.4×10 ⁻⁵
202	636.9–637.3	0	0	100	400–800	3.9	4.0×10 ⁻⁴	1.0×10 ⁻⁴
					800–1,600	1.8	1.3×10 ⁻⁴	7.2×10 ⁻⁵
204	713.1–713.4	0	0	100	200–400	72.3	3.6×10 ⁻³	5.0×10 ⁻⁵
					400–800	15.3	8.9×10 ⁻⁴	5.8×10 ⁻⁵
					800–1,600	11.0	4.1×10 ⁻⁴	3.7×10 ⁻⁵
206	859.7–860.1	0	60	40	800–1,600	122.6	4.6×10 ⁻³	3.8×10 ⁻⁵
207	901.7–902.1	0	0	100	100–200	30.7	3.0×10 ⁻³	9.8×10 ⁻⁵
					200–400	6.6	4.9×10 ⁻⁴	7.4×10 ⁻⁵
					400–800	3.5	2.0×10 ⁻⁴	5.7×10 ⁻⁵
208	972.0–972.4	0	0	100	800–1,600	1.6	6.1×10 ⁻⁵	3.8×10 ⁻⁵
					200–400	50.4	3.1×10 ⁻³	6.2×10 ⁻⁵
					400–800	4.8	3.6×10 ⁻⁴	7.5×10 ⁻⁵
210	1,153.6–1,154.0	0	20	80	800–1,600	1.4	7.0×10 ⁻⁵	5.0×10 ⁻⁵
					400–800	135.8	5.1×10 ⁻³	3.8×10 ⁻⁵
					800–1,600	70.0	2.2×10 ⁻³	3.1×10 ⁻⁵
212	1,237.7–1,238.1	0	0	100	400–800	8.1	2.7×10 ⁻⁴	3.3×10 ⁻⁵
					800–1,600	2.2	8.3×10 ⁻⁵	3.8×10 ⁻⁵
217	1,511.3–1,511.7	0	20	80	800–1,600	10.3	3.3×10 ⁻⁴	3.2×10 ⁻⁵
219	1,631.7–1,632.1	0	0	100	800–1,600	65.7	2.0×10 ⁻³	3.0×10 ⁻⁵
221	1,792.3–1,792.7	0	15	85	800–1,600	28.5	7.4×10 ⁻⁴	2.6×10 ⁻⁵
222	1,871.8–1,872.2	0	0	100	800–1,600	16.6	5.5×10 ⁻⁴	3.3×10 ⁻⁵
223	1,952.6–1,953.0	0	0	100	800–1,600	72.3	1.0×10 ⁻³	1.4×10 ⁻⁵
235	563.3–563.7	—	—	—	200–400	21.9	2.0×10 ⁻³	9.1×10 ⁻⁵
					400–800	5.7	4.3×10 ⁻⁴	7.5×10 ⁻⁵
					800–1,600	1.3	6.1×10 ⁻⁵	4.7×10 ⁻⁵

Table 3. Consolidation test summaries—Continued

Core sample No.	Depth interval (ftbls)	Gravel >4.76 mm (percent)	Sand, 4.76–0.074 mm (percent)	Silt and clay <0.074mm (percent)	Load range (lb/in ²)	c_v (ft ² /yr)	K_v (ft/yr)	S^{\wedge}_{skv} (ft ⁻¹)
Corehole 19S/17E-22J1,2 (Huron)								
Corcoran Clay Member: 730–750 ftbls								
23L181	311.5–311.9	0	5	95	50–100	30.9	7.2×10^{-3}	2.3×10^{-4}
					100–200	15.6	2.6×10^{-3}	1.7×10^{-4}
					200–400	11.5	1.3×10^{-3}	1.1×10^{-4}
					400–800	3.6	2.8×10^{-4}	7.8×10^{-5}
182	554.4–554.8	0	10	90	800–1,600	111.7	4.7×10^{-3}	8.4×10^{-5}
183	734.6–734.9	0	5	95	400–800	52.6	4.4×10^{-3}	8.4×10^{-5}
					800–1,600	21.9	1.1×10^{-3}	5.0×10^{-5}
184	904.9–905.3	0	10	90	200–400	26.3	2.0×10^{-3}	7.6×10^{-5}
					400–800	7.4	4.8×10^{-4}	6.5×10^{-5}
					800–1,600	2.6	1.3×10^{-4}	5.0×10^{-5}
185	1,093.4–1,093.8	0	20	80	800–1,600	61.3	2.6×10^{-3}	4.2×10^{-5}
186	1,251.0–1,251.4	0	15	85	400–800	11.6	5.9×10^{-4}	5.1×10^{-5}
					800–1,600	4.4	1.5×10^{-4}	3.4×10^{-5}
187	1,345.2–1,345.6	0	40	60	800–1,600	26.3	8.9×10^{-4}	3.4×10^{-5}
190	1,749.6–1,750.0	0	0	100	800–1,600	28.5	6.9×10^{-4}	2.4×10^{-5}
191	1,955.9–1,956.3	0	10	90	800–1,600	35.0	8.3×10^{-4}	2.4×10^{-5}
192	2,021.0 (–)	0	10	90	800–1,600	10.4	2.9×10^{-4}	2.8×10^{-5}
Corehole 23S/25E-16N1 (Pixley)								
Corcoran Clay Member: 280–296 ftbls								
23L226	261.7–261.9	0	55	45	200–400	311.0	2.4×10^{-2}	7.7×10^{-5}
					400–800	162.1	6.5×10^{-3}	4.0×10^{-5}
227	283.5–283.9	0	10	90	200–400	9.9	9.0×10^{-4}	9.1×10^{-5}
					400–800	4.2	4.8×10^{-4}	1.1×10^{-4}
228	292.0–292.4	0	20	80	200–400	192.7	3.2×10^{-2}	1.7×10^{-4}
					400–800	102.9	1.1×10^{-2}	1.1×10^{-4}
229	450.1–450.5	0	5	95	300–600	4.8	5.8×10^{-4}	1.2×10^{-4}
					600–1,200	2.9	1.6×10^{-4}	5.5×10^{-5}
Corehole 24S/26E-36A2 (Delano)								
Corcoran Clay Member: nonexistent								
23L237	157.1–157.4	0	80	20	400–800	55.9	3.5×10^{-3}	6.3×10^{-5}
239	443.0–443.2	0	70	30	400–800	120.7	7.7×10^{-3}	6.4×10^{-5}
240	516.0–516.3	0	20	80	400–800	24.5	1.6×10^{-3}	6.5×10^{-5}
241	607.2–607.5	0	20	80	800–1,600	120.7	4.2×10^{-3}	3.5×10^{-5}
242	725.6–725.9	0	15	85	800–1600	71.2	3.5×10^{-3}	4.9×10^{-5}
243	843.0–843.3	0	0	100	800–1,600	6.6	4.8×10^{-4}	7.3×10^{-5}
244	916.1–916.4	0	5	95	800–1,600	4.8	2.9×10^{-4}	6.0×10^{-5}
246	1,115.7–1,116.1	0	20	80	800–1,600	6.4	6.1×10^{-4}	9.5×10^{-5}
247	1,155.1–1,155.4	0	5	95	800–1,600	12.5	9.6×10^{-4}	7.7×10^{-5}

Table 3. Consolidation test summaries—Continued

Core sample No.	Depth interval (ftbls)	Gravel >4.76 mm (percent)	Sand, 4.76–0.074 mm (percent)	Silt and clay <0.074mm (percent)	Load range (lb/in ²)	c_v (ft ² /yr)	K_v (ft/yr)	S^{\wedge}_{skv} (ft ⁻¹)
Corehole 24S/26E-36A2 (Delano) Corcoran Clay Member: nonexistent —Continued								
248	1,241.0–1,241.3	0	5	95	800–1,600	7.2	7.9×10^{-4}	1.1×10^{-4}
249	1,362.3–1,362.7	0	5	95	800–1,600	5.6	4.1×10^{-4}	7.3×10^{-5}
250	1,447.4–1,447.8	0	10	90	800–1,600	4.5	4.1×10^{-4}	9.1×10^{-5}
251	1,526.2–1,526.6	0	10	90	800–1,600	1.5	8.4×10^{-5}	5.6×10^{-5}
252	1,687.0–1,687.3	0	0	100	800–1,600	18.1	6.1×10^{-5}	3.4×10^{-6}
253	1,826.2–1,826.5	0	0	100	400–800	15.4	4.3×10^{-4}	2.8×10^{-5}
					800–1,600	2.5	1.0×10^{-4}	4.0×10^{-5}

interval of 405 ft from 246 to 278 ft, which decreased the estimated specific storage from his original calculations (table 4) (Helm, 1975). However, in the digital model, Helm (1975) used the larger aquitard parameter values originally computed by Riley (1969) with the larger estimate of aquitard thickness; Helm (1975) noted this inconsistent relation.

Simulated compaction using constant parameters computed by Riley (1969) ($S'_{skv} = 2.3 \times 10^{-4} \text{ ft}^{-1}$, $S'_{ske} = 4.6 \times 10^{-6} \text{ ft}^{-1}$, $K'_v = 3.0 \times 10^{-3} \text{ ft/yr}$, and aquitard thickness = 278 ft) (table 4) agreed well with the measured compaction (Helm, 1975). Because Riley's (1969) stress-strain graphical method gives the average value of aquifer-system elastic skeletal specific storage ($2.8 \times 10^{-6} \text{ ft}^{-1}$) only, a characteristic value for aquitard elastic skeletal specific storage is somewhat arbitrary, but cannot be larger than $4.6 \times 10^{-6} \text{ ft}^{-1}$ assuming the compressibility of the aquifer-system is much smaller than the compressibility of the aquitards (Helm, 1975).

Using stress-dependent parameters, Helm (1976) simulated compaction for a 12-year period and estimated that vertical hydraulic conductivity (K'_v) decreased from about $3.4 \times 10^{-3} \text{ ft/yr}$ near the midplane of an idealized aquitard to about $3.0 \times 10^{-4} \text{ ft/yr}$ near the drainage faces of the idealized aquitard and equaled about $2.5 \times 10^{-3} \text{ ft/yr}$ when the model was calibrated to compaction without expansion (table 4). Additionally, Helm's (1976) simulations indicated that the average aquitard inelastic skeletal specific storage decreased from about 2.3×10^{-4} to $1.9 \times 10^{-4} \text{ ft}^{-1}$, corresponding to a decrease in aquitard inelastic skeletal storage coefficient from about 6.4×10^{-2} to 5.3×10^{-2} (eq. 3). The average aquitard elastic skeletal specific storage for both simulations (calibrated using constant parameters

or stress-dependent parameters) was about $4.6 \times 10^{-6} \text{ ft}^{-1}$, which corresponds to an average aquitard elastic skeletal storage coefficient of about 1.3×10^{-3} (table 4) (Helm, 1975, 1976, 1977).

The simulated compaction using stress-dependent parameters more closely matched measured compaction than did simulated compaction using constant parameters. However, Helm (1977) demonstrated that carefully evaluated values of vertical hydraulic conductivity and inelastic specific storage can be used to predict aquifer-system behavior with reasonable accuracy over several decades. Therefore, using constant parameters and the aquitard-drainage model developed for each site, Helm (1978) simulated one-dimensional compaction at seven sites in the San Joaquin Valley (table 4). Aquitard inelastic skeletal specific-storage values ranged from about 1.4×10^{-4} to $6.7 \times 10^{-4} \text{ ft}^{-1}$, and have a mean and standard deviation of about $3.2 \times 10^{-4} \text{ ft}^{-1}$ and $1.8 \times 10^{-4} \text{ ft}^{-1}$, respectively (Helm, 1978; Ireland and others, 1984). This range corresponds to aquitard inelastic skeletal storage coefficients that range from about 5×10^{-2} to 4.0×10^{-1} (Bull, 1975). Aquitard elastic skeletal specific storage values ranged from about 2.0×10^{-6} to $7.5 \times 10^{-6} \text{ ft}^{-1}$, and have a mean and standard deviation of about 4.5×10^{-6} and $2.1 \times 10^{-6} \text{ ft}^{-1}$, respectively (Helm, 1978; Ireland and others, 1984). The equivalent range of the aquitard elastic skeletal storage coefficient calculated using equation 3 ranges from about 1.2×10^{-3} to 2.6×10^{-3} . Vertical hydraulic conductivity of the aquitards ranged from about 2.0×10^{-5} to $3.0 \times 10^{-3} \text{ ft/yr}$, and have a mean and standard deviation of 7.8×10^{-4} and $1.0 \times 10^{-3} \text{ ft/yr}$, respectively (Helm, 1978; Ireland and others, 1984).

Table 4. Aquifer-system properties estimated from results of calibrated models, San Joaquin Valley, California

[State well No.: See Well-Numbering System on p. IV. See figure 1 for location of wells. S^*_{ske} , aquifer-system elastic skeletal specific storage coefficient; S'_{ske} , aquitard elastic skeletal specific storage; S_{ske} , aquifer elastic skeletal specific storage; K'_v , aquitard vertical

State well No.	Aggregate aquitard thickness (ft)	Combined thickness of aquitards and aquifers (ft)	Interval of sediments (ftbls)	Corcoran Clay (ftbls)	S^*_{ske} (ft ⁻¹)	S'_{kv}	S'_{skv} (ft ⁻¹)
San Joaquin Valley							
23S/25E-16N	246	405	355–760	¹ 274–302	2.8×10^{-6}	25.6×10^{-2}	2.3×10^{-4}
Do.	278	do.	do.	do.	—	—	2.0×10^{-4}
Do.	do.	do.	do.	do.	—	26.4×10^{-2}	2.3×10^{-4}
Do.	do.	do.	do.	do.	—	25.3×10^{-2}	1.9×10^{-4}
Do.	do.	do.	do.	do.	—	—	—
11N/21W-3B1	367	670	—	—	—	9×10^{-2}	2.5×10^{-4}
14S/13E-11D3,6	274	578	⁴ 780–1,358	⁴ 625–700	—	1.2×10^{-1}	4.3×10^{-4}
16S/15E-34N4	876	1,297	⁴ 703–3,000	⁴ 565–575	—	2.1×10^{-1}	2.4×10^{-4}
18S/19E-20P2	154	417	⁴ above 578	⁴ 567–634	—	1.0×10^{-1}	6.7×10^{-4}
19S/16E-23P2	1,324	1,960	⁴ above 3,300	⁴ not present	—	4.0×10^{-1}	3.0×10^{-4}
20S/18E-11Q1	388	620	⁴ above 710	⁴ 715–745	—	5×10^{-2}	1.4×10^{-4}
23S/25E-16N3	278	405	⁴ 355–760	¹ 274–302	—	6×10^{-2}	2.3×10^{-4}
Central Valley							
(⁵)	—	—	—	—	3.0×10^{-6}	—	3.0×10^{-4}
(⁵)	—	—	—	—	—	—	—
(⁵)	—	—	—	—	—	—	—
(⁵)	—	—	—	—	—	—	1.4×10^{-4}
(⁵)	—	—	—	—	—	—	6.7×10^{-4}
(⁵)	—	—	—	—	—	—	3.0×10^{-4}
(⁵)	300	—	—	—	—	5×10^{-2}	2×10^{-4}
(⁵)	—	—	—	—	3.0×10^{-6}	—	—

¹Riley and McClelland, 1971.²Calculated by multiplying S'_{skv} by aggregate aquitard thickness.³Calculated by multiplying S'_{ske} by aggregate aquitard thickness.⁴Bull, 1975.⁵All values for the Central Valley represent average values used in the Regional Aquifer System Analysis (RASA) model of the valley. Specific values used in the model are given in table 5.

storage; S'_{kv} , aquitard inelastic skeletal storage coefficient; S'_{skv} , aquitard inelastic skeletal specific storage; S'_{ke} , aquitard elastic skeletal hydraulic conductivity. ft, foot; ftbls, feet below land surface; ft^{-1} , per foot; ft/yr, foot per year; —, not reported]

S'_{ke}	S'_{ske} (ft^{-1})	S_{ske} (ft^{-1})	K'_v (ft/yr)	Reference	Comments
San Joaquin Valley					
1.1×10^{-3}	4.6×10^{-6}	—	3.0×10^{-3}	Helm, 1975	S^*_{ske} value assumes compressibility of aquifer skeleton and aquitard skeleton are equivalent.
—	4.1×10^{-6}	—		do.	Revised estimate of aggregate aquitard thickness was based on reevaluated electric logs and micrologs by F.S. Riley.
1.3×10^{-3}	4.6×10^{-6}	—	3.4×10^{-3}	Helm, 1976, 1977	S'_{skv} , maximum of range reported; K'_v , maximum of range reported.
—	—	—	3.0×10^{-4}	do.	S'_{skv} , minimum of range reported; K'_v , minimum of range reported.
—	—	—	2.5×10^{-3}	do.	K'_v from calibration to compaction without expansion.
$^3 1.5 \times 10^{-3}$	4.0×10^{-6}	4.3×10^{-7}	3.0×10^{-4}	Helm, 1978; Ireland and others, 1984	
$^3 1.9 \times 10^{-3}$	7.0×10^{-6}	do.	7.7×10^{-4}	do.	
$^3 1.9 \times 10^{-3}$	2.2×10^{-6}	do.	5.2×10^{-4}	do.	
$^3 1.2 \times 10^{-3}$	7.5×10^{-6}	do.	7.0×10^{-4}	do.	
$^3 2.6 \times 10^{-3}$	2.0×10^{-6}	do.	2.0×10^{-5}	do.	
$^3 1.6 \times 10^{-3}$	4.0×10^{-6}	do.	1.2×10^{-4}	do.	
$^3 1.3 \times 10^{-3}$	4.6×10^{-6}	do.	3.0×10^{-3}	do.	
Central Valley					
—	4.6×10^{-6}	9.1×10^{-7}	—	Prudic and Williamson, 1986	Estimates obtained from Poland (1961), Helm (1978), and Ireland and others (1984).
—		7×10^{-7}	—	Williamson and others, 1989	Minimum value of range reported by Riley and McClelland (1971).
—		1×10^{-6}	—	do.	Maximum value of range reported by Riley and McClelland (1971).
—	2.0×10^{-6}	—	—	do.	Minimum value of range reported by Helm (1978).
—	7.5×10^{-6}	—	—	do.	Maximum value of range reported by Helm (1978).
—	—	—	—	do.	Mean value of range reported by Helm (1978).
—	—	1.4×10^{-6}	—	do.	Values obtained from Poland (1961).
—	4.5×10^{-6}	1.0×10^{-6}	—	do.	S^*_{ske} represents about half fine-grained and half coarse-grained sediment.

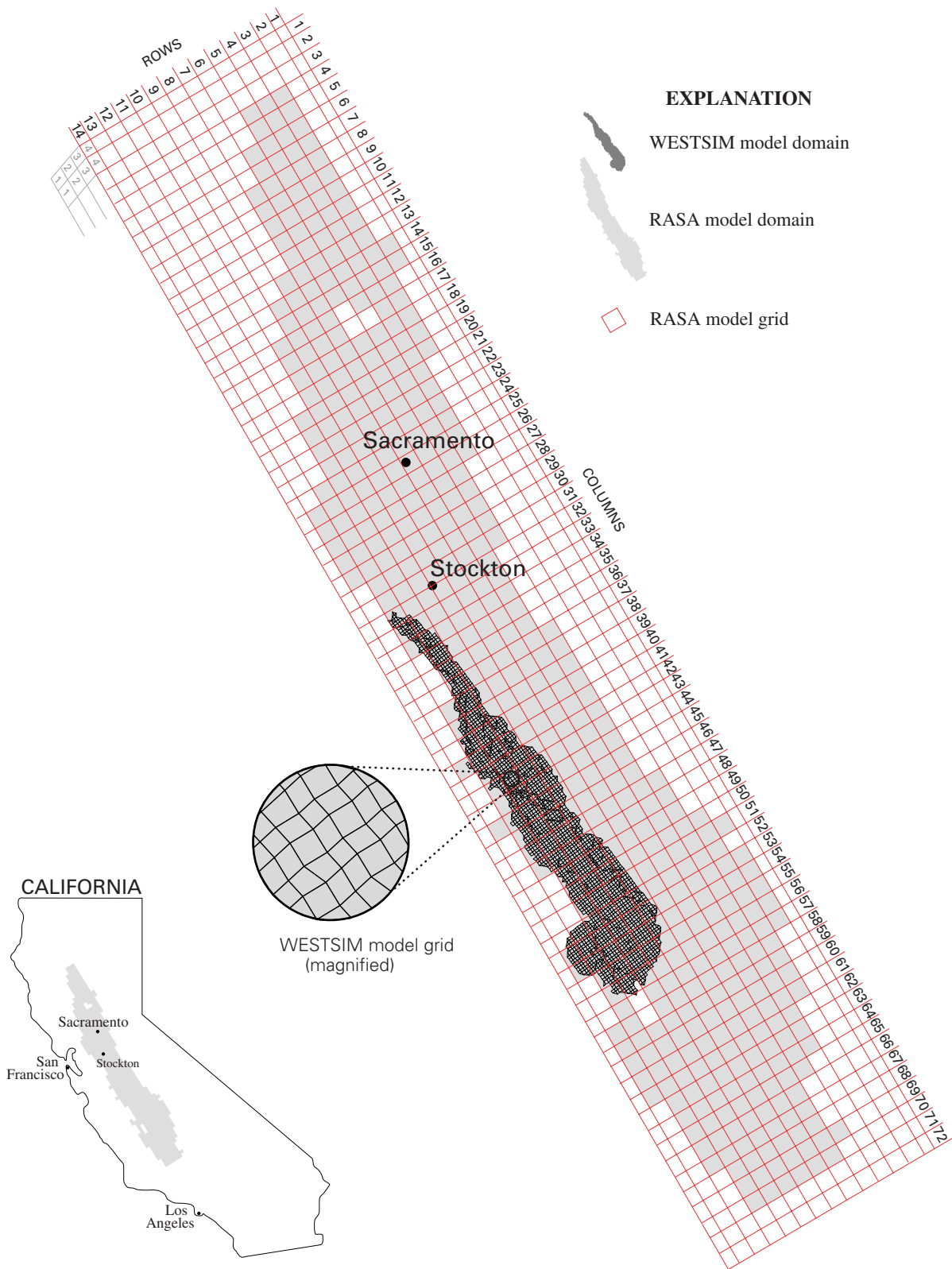


Figure 2. Relation of WESTSIM (U.S. Bureau of Reclamation) model domain and RASA (U.S. Geological Survey) model domain.

Prudic and Williamson (1986) and Williamson and others (1989) used a three-dimensional model as part of the U.S. Geological Survey's Regional Aquifer-System Analysis (RASA) program to simulate ground-water flow and aquifer-system compaction (land subsidence) in the Central Valley. The geographic relation of the RASA model domain and the WESTSIM model domain is shown in figure 2. Prudic and Williamson (1986) evaluated the modeling technique, and Williamson and others (1989) documented the calibrated model. The storage values reported in the two papers are inconsistent because the model was in developmental stages when the first paper was published; both papers, in terms of storage properties reported, are summarized separately here.

Prudic and Williamson (1986) reported that initial estimates of elastic and inelastic skeletal specific storages were obtained from Poland (1961), Helm (1978), and Ireland and others (1984) (table 4). Elastic skeletal specific storage of the coarse- (S_{ske}) and the fine-grained (S'_{ske}) deposits in the Central Valley were estimated as 9.1×10^{-7} and 4.6×10^{-6} ft⁻¹, respectively, and the combined average of elastic skeletal specific storage for a sample that has a slight majority of fine-grained deposits was estimated as 3×10^{-6} ft⁻¹. The inelastic skeletal specific storage of fine-grained deposits (S'_{skv}) was estimated as 3×10^{-4} ft⁻¹ (Prudic and Williamson, 1986).

Williamson and others (1989) reported that initial values of elastic skeletal specific storage of the coarse-grained deposits were based on values reported by Poland (1961), 1.4×10^{-6} ft⁻¹, and by Riley and McClelland (1971), which ranged from about 7×10^{-7} to 1×10^{-6} ft⁻¹ (table 4). Initial estimates of elastic skeletal specific storage of the fine-grained deposits (S'_{ske}) were based on values obtained from model results that Helm (1978) reported, which ranged from about 2.0×10^{-6} to 7.5×10^{-6} ft⁻¹ and averaged about 4.5×10^{-6} ft⁻¹. Williamson and others (1989) initially used elastic skeletal specific-storage values of about 1×10^{-6} ft⁻¹ for parts of the aquifer system that are all coarse-grained, about 4.5×10^{-6} ft⁻¹ for parts that are all fine grained, and about 3×10^{-6} ft⁻¹ for parts that are half coarse grained and half fine grained (table 4).

Estimates of aquitard inelastic skeletal storage coefficients were calculated by estimating the

thickness of fine-grained beds in the aquifer system and multiplying that value by the mean aquitard inelastic skeletal specific-storage value of about 3×10^{-4} ft⁻¹, calculated by Helm (1978), who estimated aquitard inelastic skeletal specific-storage values at seven sites in the San Joaquin Valley where the values ranged from about 1.4×10^{-4} to 6.7×10^{-4} ft⁻¹ (Williamson and others, 1989). Another estimate of the aquitard inelastic skeletal specific-storage value considered was about 2×10^{-4} ft⁻¹, calculated by Poland (1961) assuming a 300-ft-thick clayey section in the aquifer system and a computed aquitard inelastic skeletal storage coefficient of about 5×10^{-2} (table 4). The value of inelastic skeletal specific storage calculated by Poland (1961) is reasonably close to the mean estimated by Helm (1978).

During model calibration, elastic skeletal specific-storage values generally were increased by a factor of 2, except in the Los Banos–Kettleman City area where the value was not changed. The increase was needed to reduce the simulated water-level fluctuations caused by alternating periods of seasonal recharge and discharge; allocating all agricultural pumpage to the autumn period and all recharge to the spring period exaggerated the seasonal change in stress. Aquitard inelastic skeletal specific-storage values in the model simulations were adjusted very little during model calibration. A subset of appendix B from Williamson and others (1989), corresponding to geographically coincident areas covered by the WESTSIM model (fig. 2), is presented in table 5. Values in table 5 include the column/row coordinates of the RASA model, sediment thickness of each cell for each layer, percentage of fine-grained sediment for each layer, and aggregate aquitard thicknesses, aquitard inelastic skeletal storage coefficients, and equivalent aquitard inelastic skeletal specific storages for layers 2 and 3; aquifer-system compaction was not simulated in layers 1, the lowest layer, and 4, the highest layer. The aquitard inelastic skeletal specific storages were computed for each column/row coordinate in layers 2 and 3 by dividing the inelastic storage coefficient by the aggregate thickness of fine-grained sediment for that column/row coordinate for each of the two layers (eq. 3) (table 5).

Table 5. Aquifer-system properties used in Regional Aquifer-System Analysis simulations

[Table modified from appendix B in Williamson and others, 1989. Locations of columns and rows are shown in figure 2. Layer 1 is lowest model layer. Values of aquitard inelastic skeletal specific storage (S'_{skv}) for layers 2 and 3 were calculated by dividing the aquitard inelastic skeletal storage coefficient (S'_{kv}) by the aggregate thickness of fine-grained sediments for layers 2 and 3, respectively. ft^{-1} , per foot; —, no data; na, not applicable]

Column	Row	Sediment thickness, in feet				Percentage of fine-grained sediment				Aggregate thickness of fine-grained sediments, in feet		S'_{kv} (layers 2 and 3)	S'_{skv}	
		Layer 1	Layer 2	Layer 3	Layer 4	Layer 1	Layer 2	Layer 3	Layer 4	Layer 2	Layer 3		Layer 2 (ft^{-1})	Layer 3 (ft^{-1})
32	8	1,050	250	250	300	100	44	37	57	110	92.5	2.5×10^{-2}	2.3×10^{-4}	2.7×10^{-4}
32	9	1,780	200	300	300	100	44	37	57	88	111.0	3.0×10^{-2}	3.4×10^{-4}	2.7×10^{-4}
32	10	2,300	320	300	280	100	44	37	57	140.8	111.0	4.4×10^{-2}	3.1×10^{-4}	4.0×10^{-4}
32	11	3,200	200	400	200	—	64	56	62	128	224.0	4.4×10^{-2}	3.4×10^{-4}	2.0×10^{-4}
32	12	2,600	350	300	150	—	64	56	62	224	168.0	5.3×10^{-2}	2.4×10^{-4}	3.2×10^{-4}
33	8	582	600	300	288	100	44	37	57	264	111.0	7.3×10^{-2}	2.8×10^{-4}	6.6×10^{-4}
33	9	1,390	650	300	250	100	44	37	57	286	111.0	9.3×10^{-2}	3.3×10^{-4}	8.4×10^{-4}
33	10	2,350	800	200	173	—	64	56	62	512	112.0	7.8×10^{-2}	1.5×10^{-4}	7.0×10^{-4}
33	11	2,500	500	493	232	—	64	56	62	320	276.1	1.1×10^{-1}	3.4×10^{-4}	4.0×10^{-4}
33	12	2,000	500	485	185	—	64	56	62	320	271.6	8.2×10^{-2}	2.6×10^{-4}	3.0×10^{-4}
34	8	885	275	425	300	100	44	37	57	121	157.3	5.1×10^{-2}	4.2×10^{-4}	3.2×10^{-4}
34	9	1,760	550	250	200	100	44	37	57	242	92.5	6.2×10^{-2}	2.6×10^{-4}	6.7×10^{-4}
34	10	2,380	600	250	150	100	44	37	57	264	92.5	7.8×10^{-2}	3.0×10^{-4}	8.4×10^{-4}
34	11	2,410	400	500	115	100	44	37	57	176	185.0	6.8×10^{-2}	3.9×10^{-4}	3.7×10^{-4}
34	12	1,480	400	500	45	—	64	56	62	256	280.0	8.0×10^{-2}	3.1×10^{-4}	2.9×10^{-4}
35	8	295	1,000	400	300	—	—	—	—	na	na	1.1×10^{-1}	—	—
35	9	1,350	1,200	224	200	100	44	37	57	528	82.9	1.2×10^{-1}	2.3×10^{-4}	1.4×10^{-3}
35	10	1,480	1,300	320	140	—	—	—	—	na	na	1.4×10^{-1}	—	—
35	11	1,360	900	700	192	—	64	56	62	576	392.0	1.9×10^{-1}	3.3×10^{-4}	4.8×10^{-4}
36	8	580	800	310	300	—	—	—	—	na	na	9.7×10^{-2}	—	—
36	9	1,320	1,100	250	161	—	—	—	—	na	na	1.2×10^{-1}	—	—
36	10	1,540	1,200	350	135	—	—	—	—	na	na	1.4×10^{-1}	—	—
36	11	1,540	900	700	172	—	—	56	67	na	392.0	1.4×10^{-1}	—	3.6×10^{-4}
37	8	1,120	450	300	250	—	—	—	—	na	na	6.6×10^{-2}	—	—
37	9	1,780	700	150	149	—	—	—	—	na	na	7.6×10^{-2}	—	—
37	10	2,300	600	250	165	—	—	—	—	na	na	7.6×10^{-2}	—	—
37	11	1,590	575	480	219	—	—	56	67	na	268.8	9.0×10^{-2}	—	3.3×10^{-4}
38	8	1,150	700	320	200	—	—	—	—	na	na	8.9×10^{-2}	—	—

Table 5. Aquifer-system properties used in Regional Aquifer-System Analysis simulations—Continued

Column	Row	Sediment thickness, in feet				Percentage of fine-grained sediment				Aggregate thickness of fine-grained sediments, in feet		S'_{kv} (layers 2 and 3)	S'_{skv}		
		Layer 1	Layer 2	Layer 3	Layer 4	Layer 1	Layer 2	Layer 3	Layer 4	Layer 2	Layer 3		Layer 2 (ft ⁻¹)	Layer 3 (ft ⁻¹)	
	38	9	1,900	900	200	143	—	—	—	—	na	na	9.7×10^{-2}	—	—
	38	10	2,140	800	200	234	—	—	—	—	na	na	8.7×10^{-2}	—	—
	38	11	2,230	500	350	178	—	—	56	67	na	196.0	7.1×10^{-2}	—	3.6×10^{-4}
	38	12	0	50	100	200	—	—	56	67	na	56.0	6.6×10^{-3}	—	1.2×10^{-4}
	39	8	1,620	450	310	200	—	—	—	—	na	na	6.4×10^{-2}	—	—
	39	9	2,210	600	250	104	—	—	—	—	na	na	7.3×10^{-2}	—	—
	39	10	2,390	550	250	202	—	—	—	—	na	na	6.7×10^{-2}	—	—
	39	11	1,910	600	440	243	—	—	56	67	na	246.4	8.3×10^{-2}	—	3.4×10^{-4}
	39	12	0	50	200	170	—	—	56	67	na	112.0	1.1×10^{-2}	—	9.8×10^{-5}
	40	8	1,790	500	200	100	—	—	—	—	na	na	5.7×10^{-2}	—	—
	40	9	2,580	550	100	151	—	—	—	—	na	na	5.4×10^{-2}	—	—
	40	10	2,770	550	100	192	—	—	—	—	na	na	5.2×10^{-2}	—	—
	40	11	2,360	350	250	251	—	—	56	67	na	140.0	4.6×10^{-2}	—	3.3×10^{-4}
	40	12	0	100	200	80	—	—	56	67	na	112.0	1.8×10^{-2}	—	1.6×10^{-4}
	41	8	1,820	400	290	95	—	—	—	—	na	na	5.5×10^{-2}	—	—
	41	9	2,530	400	250	159	—	—	—	—	na	na	5.2×10^{-2}	—	—
	41	10	2,940	300	200	185	—	—	56	67	na	112.0	3.8×10^{-2}	—	3.4×10^{-4}
	41	11	2,240	350	250	235	—	—	56	67	na	140.0	4.4×10^{-2}	—	3.1×10^{-4}
	41	12	487	350	200	248	—	—	56	67	na	112.0	3.7×10^{-2}	—	3.3×10^{-4}
	41	13	0	50	100	100	—	—	56	67	na	56.0	6.3×10^{-3}	—	1.1×10^{-4}
	42	8	1,480	840	200	141	—	—	—	—	na	na	8.2×10^{-2}	—	—
	42	9	2,240	500	420	181	—	—	—	—	na	na	7.1×10^{-2}	—	—
	42	10	2,560	450	400	21	—	—	56	67	na	224.0	6.3×10^{-2}	—	2.8×10^{-4}
	42	11	1,940	450	396	255	—	—	56	67	na	221.8	8.4×10^{-2}	—	3.8×10^{-4}
	42	12	16	500	355	219	—	—	56	67	na	198.8	6.3×10^{-2}	—	3.2×10^{-4}
	43	8	1,200	800	340	136	—	—	—	—	na	na	8.9×10^{-2}	—	—
	43	9	1,890	500	600	206	—	—	—	—	na	na	8.4×10^{-2}	—	—
	43	10	2,340	800	100	237	—	—	56	67	na	56.0	9.0×10^{-2}	—	1.6×10^{-3}
	43	11	720	600	297	291	—	—	56	67	na	166.3	8.6×10^{-2}	—	5.2×10^{-4}
	43	12	0	500	508	143	—	—	56	67	na	284.5	7.8×10^{-2}	—	2.7×10^{-4}
	44	8	1,800	400	400	151	—	—	62	66	na	248.0	9.5×10^{-2}	—	3.8×10^{-4}
	44	9	1,540	800	600	209	—	—	62	66	na	372.0	1.4×10^{-1}	—	3.8×10^{-4}
	44	10	1,690	1,000	395	239	—	—	56	67	na	221.2	1.3×10^{-1}	—	5.9×10^{-4}
	44	11	1,120	765	500	328	—	—	56	67	na	280.0	1.2×10^{-1}	—	4.3×10^{-4}
	44	12	0	400	440	1	—	—	56	67	na	246.4	6.5×10^{-2}	—	2.6×10^{-4}

Estimates of Aquifer-System Storage Values 21

Table 5. Aquifer-system properties used in Regional Aquifer-System Analysis simulations—Continued

Column	Row	Sediment thickness, in feet				Percentage of fine-grained sediment				Aggregate thickness of fine-grained sediments, in feet		S'_{kv} (layers 2 and 3)	S'_{skv}		
		Layer 1	Layer 2	Layer 3	Layer 4	Layer 1	Layer 2	Layer 3	Layer 4	Layer 2	Layer 3		Layer 2 (ft ⁻¹)	Layer 3 (ft ⁻¹)	
	45	8	2,160	250	660	189	—	—	62	66	na	409.2	1.0×10^{-1}	—	2.4×10^{-4}
	45	9	2,400	325	520	258	—	—	56	67	na	291.2	8.0×10^{-2}	—	2.7×10^{-4}
	45	10	2,080	500	500	306	—	—	56	67	na	280.0	1.0×10^{-1}	—	3.6×10^{-4}
	45	11	1,340	500	410	364	—	—	56	67	na	229.6	4.8×10^{-2}	—	2.1×10^{-4}
	45	12	0	300	270	1	—	—	56	67	na	151.2	4.3×10^{-2}	—	2.8×10^{-4}
	45	13	0	50	100	1	—	—	56	67	na	56.0	1.1×10^{-2}	—	2.0×10^{-4}
	46	8	1,970	700	600	263	—	—	62	66	na	372.0	1.1×10^{-1}	—	3.0×10^{-4}
	46	9	2,170	900	265	299	—	—	56	67	na	148.4	1.1×10^{-1}	—	7.4×10^{-4}
	46	10	2,540	600	500	375	—	—	56	67	na	280.0	5.4×10^{-2}	—	1.9×10^{-4}
	46	11	1,630	600	598	295	—	—	56	67	na	334.9	5.1×10^{-2}	—	1.5×10^{-4}
	46	12	0	775	600	1	—	—	56	67	na	336.0	1.4×10^{-1}	—	4.2×10^{-4}
	47	8	2,190	1,100	415	325	—	70	50	62	770	207.5	1.5×10^{-1}	1.9×10^{-4}	7.2×10^{-4}
	47	9	2,300	1,100	500	342	—	—	56	67	na	280.0	8.7×10^{-2}	—	3.1×10^{-4}
	47	10	2,280	1,100	659	255	—	—	56	67	na	369.0	1.5×10^{-1}	—	4.1×10^{-4}
	47	11	1,620	1050	903	245	—	—	56	67	na	505.7	1.5×10^{-1}	—	3.0×10^{-4}
	47	12	0	920	935	187	58	59	62	65	542.8	579.7	7.7×10^{-2}	1.4×10^{-4}	1.3×10^{-4}
	48	8	3,010	800	389	364	—	70	50	62	560	194.5	6.6×10^{-2}	1.2×10^{-4}	3.4×10^{-4}
	48	9	3,740	800	307	433	—	—	56	67	na	171.9	4.0×10^{-2}	—	2.3×10^{-4}
	48	10	3,330	600	630	337	58	59	62	65	354	390.6	9.7×10^{-2}	2.7×10^{-4}	2.5×10^{-4}
	48	11	2,180	700	957	245	58	59	62	65	413	593.3	1.7×10^{-1}	4.1×10^{-4}	2.9×10^{-4}
	48	12	358	700	730	80	58	59	62	65	413	452.6	1.1×10^{-1}	2.7×10^{-4}	2.4×10^{-4}
	49	8	3,460	1,240	125	442	—	62	61	50	768.8	76.3	1.1×10^{-1}	1.4×10^{-4}	1.4×10^{-5}
	49	9	3,550	700	920	187	—	62	61	50	434	561.2	1.1×10^{-1}	2.5×10^{-4}	2.0×10^{-4}
	49	10	2,840	700	997	180	58	59	62	65	413	618.1	7.7×10^{-2}	1.9×10^{-4}	1.2×10^{-4}
	49	11	2,570	800	915	255	58	59	62	65	472	567.3	1.8×10^{-1}	3.8×10^{-4}	3.2×10^{-4}
	50	8	3,870	900	472	515	—	62	61	50	558	287.9	1.2×10^{-1}	2.2×10^{-4}	4.2×10^{-4}
	50	9	3,130	800	898	237	—	62	61	50	496	547.8	9.0×10^{-2}	1.8×10^{-4}	1.6×10^{-4}
	50	10	3,790	700	1,050	145	58	59	62	65	413	651.0	1.5×10^{-1}	3.6×10^{-4}	2.3×10^{-4}
	50	11	1,750	1,500	860	440	58	59	62	65	885	533.2	1.2×10^{-1}	1.4×10^{-4}	2.3×10^{-4}
	51	8	2,420	1,600	350	492	—	62	61	50	992	213.5	8.9×10^{-2}	9.0×10^{-5}	4.2×10^{-4}
	51	9	3,140	1,400	895	205	—	62	61	50	868	546.0	9.2×10^{-2}	1.1×10^{-4}	1.7×10^{-4}
	51	10	3,840	1,120	1,310	220	58	59	62	65	660.8	812.2	1.1×10^{-1}	1.7×10^{-4}	1.4×10^{-4}

Table 5. Aquifer-system properties used in Regional Aquifer-System Analysis simulations—Continued

Column	Row	Sediment thickness, in feet				Percentage of fine-grained sediment				Aggregate thickness of fine-grained sediments, in feet		S'_{kv} (layers 2 and 3)	S'_{skv}		
		Layer 1	Layer 2	Layer 3	Layer 4	Layer 1	Layer 2	Layer 3	Layer 4	Layer 2	Layer 3		Layer 2 (ft ⁻¹)	Layer 3 (ft ⁻¹)	
	51	11	2,230	1,410	1,180	340	58	59	62	65	831.9	731.6	1.5×10^{-1}	1.8×10^{-4}	2.1×10^{-4}
	52	8	3,500	1,200	335	505	—	62	61	50	744	204.4	1.3×10^{-1}	1.7×10^{-4}	6.4×10^{-4}
	52	9	3,700	800	1,560	175	58	59	62	65	472	967.2	2.3×10^{-1}	4.9×10^{-4}	2.4×10^{-4}
	52	10	4,360	1,000	1,580	275	58	59	62	65	590	979.6	2.4×10^{-1}	4.1×10^{-4}	2.4×10^{-4}
	52	11	2,370	1,310	1,210	320	58	59	62	65	772.9	750.2	1.9×10^{-1}	2.5×10^{-4}	2.5×10^{-4}
	53	8	4,000	1,300	260	488	—	62	61	50	806	158.6	8.1×10^{-2}	1.0×10^{-4}	5.1×10^{-4}
	53	9	4,870	700	1,060	240	58	59	62	65	413	657.2	1.7×10^{-1}	4.1×10^{-4}	2.6×10^{-4}
	53	10	5,200	800	1,260	210	58	59	62	65	472	781.2	1.9×10^{-1}	4.0×10^{-4}	2.4×10^{-4}
	53	11	3,120	900	1,100	345	58	59	62	65	531	682.0	1.4×10^{-1}	2.6×10^{-4}	2.1×10^{-4}
	53	13	0	0	100	100	69	48	23	47	0	23.0	0	—	0
	54	8	3,010	800	800	515	—	62	61	50	496	488.0	4.5×10^{-2}	9.1×10^{-5}	9.2×10^{-5}
	54	9	1,200	700	912	480	58	59	62	65	413	565.4	1.0×10^{-1}	2.4×10^{-4}	1.8×10^{-4}
	54	10	965	700	1,060	295	58	59	62	65	413	657.2	1.3×10^{-1}	3.1×10^{-4}	2.0×10^{-4}
	54	11	945	700	995	280	69	48	23	47	336	228.9	1.2×10^{-1}	3.6×10^{-4}	5.2×10^{-4}
	54	12	252	500	958	270	69	48	23	47	240	220.3	8.7×10^{-2}	3.6×10^{-4}	3.9×10^{-4}
	54	13	0	0	50	50	69	48	23	47	0	11.5	0	—	0
	55	8	1,560	700	768	532	74	50	42	57	350	322.6	9.4×10^{-2}	2.7×10^{-4}	2.9×10^{-4}
	55	9	522	800	1,120	250	58	59	62	65	472	694.4	1.5×10^{-1}	3.2×10^{-4}	2.2×10^{-4}
	55	10	910	900	1,330	225	58	59	62	65	531	824.6	1.7×10^{-1}	3.2×10^{-4}	2.1×10^{-4}
	55	11	0	1,370	1,240	290	58	59	62	65	808.3	768.8	2.5×10^{-1}	3.1×10^{-4}	3.3×10^{-4}
	55	12	0	700	1,130	110	69	48	23	47	336	259.9	1.7×10^{-1}	5.1×10^{-4}	6.5×10^{-4}
	56	8	919	850	696	555	74	50	42	57	425	292.3	9.4×10^{-2}	2.2×10^{-4}	3.2×10^{-4}
	56	9	735	850	900	650	58	59	62	65	501.5	558.0	1.1×10^{-1}	2.2×10^{-4}	2.0×10^{-4}
	56	10	885	700	1,270	360	58	59	62	65	413	787.4	8.6×10^{-2}	2.1×10^{-4}	1.1×10^{-4}
	56	12	4,520	1,000	500	100	69	48	23	47	480	115.0	1.4×10^{-1}	2.9×10^{-4}	1.2×10^{-3}
	57	8	882	700	740	560	74	50	42	57	350	310.8	7.9×10^{-2}	2.3×10^{-4}	2.5×10^{-4}
	57	9	0	600	700	700	74	50	42	57	300	294.0	8.0×10^{-2}	2.7×10^{-4}	2.7×10^{-4}
	57	10	1,120	600	650	650	74	50	42	57	300	273.0	1.1×10^{-1}	3.7×10^{-4}	4.0×10^{-4}
	57	12	3,100	500	300	440	69	48	23	47	240	69.0	8.0×10^{-2}	3.3×10^{-4}	1.2×10^{-3}

Estimates of Aquifer-System Storage Values

EVALUATION OF SPECIFIC-STORAGE VALUES

Calibrated models of aquifer-system compaction developed by Helm (1975, 1976, 1977, 1978) and by Williamson and others (1989) indicate that a narrow range of both aquitard inelastic skeletal specific storage values and aquitard elastic skeletal specific storage values have been used to successfully simulate aquifer-system compaction despite differences in depth, thickness, lithology, and stratigraphy among the San Joaquin Valley sites that were modeled (table 4). The aquitard inelastic skeletal specific storage values derived by Helm (1978) for seven sites in the San Joaquin Valley ranged from about 1.4×10^{-4} to $6.7 \times 10^{-4} \text{ ft}^{-1}$, and have a mean of about $3.2 \times 10^{-4} \text{ ft}^{-1}$ and a standard deviation of about $1.8 \times 10^{-4} \text{ ft}^{-1}$. The aquitard elastic skeletal specific storage values that Helm (1978) derived ranged from about 2.0×10^{-6} to $7.5 \times 10^{-6} \text{ ft}^{-1}$, and have a mean of about $4.5 \times 10^{-6} \text{ ft}^{-1}$ and a standard deviation of about $2.1 \times 10^{-6} \text{ ft}^{-1}$. Aquitard elastic and inelastic skeletal specific storage values used by Williamson and others (1989) fall within the ranges of values derived by Helm.

The narrow range of aquitard inelastic and elastic skeletal specific storage values derived by Helm (1978) at these seven sites also has been found elsewhere in the United States, including areas of California other than the San Joaquin Valley. For seven sites in the Santa Clara Valley, California, model-derived values of aquitard inelastic skeletal specific storage ranged from 1.4×10^{-4} to $4.0 \times 10^{-4} \text{ ft}^{-1}$ (Helm, 1978) and have a mean of $2.8 \times 10^{-4} \text{ ft}^{-1}$ and a standard deviation of $8.9 \times 10^{-5} \text{ ft}^{-1}$. The model-derived values of aquitard elastic skeletal specific storage for the seven Santa Clara Valley sites ranged from 2.2×10^{-6} to $1.6 \times 10^{-5} \text{ ft}^{-1}$ (Helm, 1978) and have a mean of $6.7 \times 10^{-6} \text{ ft}^{-1}$ and a standard deviation of $5.2 \times 10^{-6} \text{ ft}^{-1}$.

At an extensometer site in Antelope Valley in the Mojave Desert of southern California, the model-derived value of aquitard inelastic skeletal specific storage for aquitards that were actively compacting inelastically was $3.5 \times 10^{-4} \text{ ft}^{-1}$ (Sneed and Galloway, 2000), which is strikingly close to the mean value of $3.2 \times 10^{-4} \text{ ft}^{-1}$ for the 7 sites in San Joaquin Valley. At this same Antelope Valley site, the model-derived value of aquifer-system elastic skeletal specific storage was $1.7 \times 10^{-6} \text{ ft}^{-1}$ (Sneed and Galloway, 2000). This value is slightly smaller than those reported for the San Joaquin and Santa Clara Valleys, perhaps because the elastic skeletal specific storage value for the Antelope

Valley site represents an average value for the aquifer system, rather than an elastic skeletal specific storage value that explicitly represents the aquitard component of the aquifer system.

Hanson (1989) reported model-derived estimates for selected extensometer sites in the Tucson basin and in the Avra Valley using the Helm model approach. For the six Arizona sites, the model-derived values of aquitard inelastic skeletal specific storage ranged from 7.3×10^{-6} to $2.7 \times 10^{-4} \text{ ft}^{-1}$ (Hanson, 1989) and have a mean of $9.4 \times 10^{-5} \text{ ft}^{-1}$ and a standard deviation of $1.1 \times 10^{-4} \text{ ft}^{-1}$. Smaller values in this range may indicate that the aquifer systems were still in transition to predominantly inelastic compaction when the study was done; hence long-term inelastic skeletal specific-storage values may initially increase because of increased compaction through time (Hanson, 1989). The model-derived values of aquitard elastic skeletal specific storage for the six Arizona sites ranged from 1.0×10^{-6} to $2.0 \times 10^{-5} \text{ ft}^{-1}$ (Hanson, 1989) and have a mean of $7.1 \times 10^{-6} \text{ ft}^{-1}$ and a standard deviation of $6.6 \times 10^{-6} \text{ ft}^{-1}$. Epstein (1987) reported on model-derived estimates for an extensometer site near Eloy, Ariz. The model-derived value of aquitard inelastic skeletal specific storage for the upper five layers was $1.5 \times 10^{-4} \text{ ft}^{-1}$; layers 6 and 7 used 1.8×10^{-4} and $2.7 \times 10^{-4} \text{ ft}^{-1}$, respectively. The model-derived value of the aquitard elastic skeletal specific storage for layers 1 through 5 and 7 was $3.0 \times 10^{-6} \text{ ft}^{-1}$; layer 6 used $2.4 \times 10^{-6} \text{ ft}^{-1}$ (Epstein, 1987).

Inelastic skeletal specific storage measured from laboratory consolidation tests on samples tend to result in smaller values compared with those derived from calibrated models of aquifer-system compaction. At site 14S/13E-11D, the model-derived estimate of inelastic skeletal specific storage was $4.3 \times 10^{-4} \text{ ft}^{-1}$ (Helm, 1978). For the same location, laboratory consolidation tests on eight samples yielded inelastic skeletal specific storage values ranging from 2.0×10^{-5} to $1.6 \times 10^{-4} \text{ ft}^{-1}$ (Johnson and others, 1968) (table 3). The larger value was measured in a sample from the Corcoran Clay, which would be expected to be highly compressible, yet this value is smaller than Helm's (1978) derived value by a factor of about 2.7. At site 16S/15E-34N, the model-derived estimate of inelastic skeletal specific storage was $2.4 \times 10^{-4} \text{ ft}^{-1}$ (Helm, 1978). For the same location, laboratory consolidation tests on 16 samples yielded inelastic skeletal specific storage values ranging from 1.4×10^{-5} to $1.7 \times 10^{-4} \text{ ft}^{-1}$

(Johnson and others, 1968) (table 3); the largest value in this range is smaller than Helm's (1978) by a factor of about 1.4. In this example, the largest values were not measured in samples from the Corcoran Clay, but in sediments collected above the Corcoran Clay (Johnson and others, 1968) (table 3). At site 23S/25E-16N, the model-derived estimate of inelastic skeletal specific storage was $2.3 \times 10^{-4} \text{ ft}^{-1}$ (Helm, 1978). For the same location, laboratory consolidation tests of four samples yielded inelastic skeletal specific storage values ranging from 4.0×10^{-5} to $1.7 \times 10^{-4} \text{ ft}^{-1}$ (Johnson and others, 1968) (table 3). At this site, the larger value was measured in a sample from the Corcoran Clay (Johnson and others, 1968) (table 3), which would be expected to be highly compressible, yet this value is smaller than Helm's (1978) model-derived value by a factor of about 1.3. This discrepancy may result from the scale difference: laboratory consolidation tests measure a small sample of an aquifer system, whereas calibrated models focus on larger thicknesses of aquifer systems. Furthermore, laboratory consolidation tests are done with the premise that the sample is undisturbed, which is nearly impossible, and do not mimic natural stresses on, or stress history of, the sample.

SUMMARY

This report summarizes the hydraulic and mechanical properties affecting ground-water flow and aquifer-system compaction in the San Joaquin Valley, California. Because most storage values presented are components of the total aquifer-system storage and include inelastic and elastic skeletal storage values for aquifers and aquitards, the relations of components of aquifer-system storage to total aquifer-system storage were reviewed. Vertical hydraulic conductivity values generally are for discrete thicknesses of sediments—usually aquitards. The property values were obtained from publications that report the values as results of aquifer tests, stress-strain analyses of borehole extensometer observations, laboratory consolidation tests, and model simulations. These values will be used by the USBR during the calibration process of the WESTSIM model, which will simulate ground-water flow and land subsidence in the western San Joaquin Valley.

REFERENCES

- Bull, W.B., 1975, Land subsidence due to ground-water withdrawal in the Los Banos-Kettleman City area, California, Part 2. Subsidence and compaction of deposits: U.S. Geological Survey Professional Paper 437-F, 90 p.
- Bull, W.B., and Poland, J.F., 1975, Land subsidence due to ground-water withdrawal in the Los Banos-Kettleman City area, California, Part 3. Interrelations of water-level change, change in aquifer-system thickness, and subsidence: U.S. Geological Survey Professional Paper 437-G, 62 p.
- Davis, G.H., Green, J.H., Olmsted, F.H., and Brown, D.W., 1959, Ground-water conditions and storage capacity in the San Joaquin Valley, California: U.S. Geological Survey Water-Supply Paper 1469, 287 p., 29 pls.
- Epstein, V.J., 1987, Hydrologic and geologic factors affecting land subsidence near Eloy, Arizona: U.S. Geological Survey Water-Resources Investigations Report 87-4143, 28 p.
- Hanson, R.T., 1989, Aquifer-system compaction, Tucson Basin and Avra Valley, Arizona: U.S. Geological Survey Water-Resources Investigations Report 88-4172, 69 p.
- Helm, D.C., 1975, One-dimensional simulation of aquifer system compaction near Pixley, California—1. Constant parameters: *Water Resources Research*, v. 11, no. 3, p. 465–478.
- , 1976, One-dimensional simulation of aquifer system compaction near Pixley, California—2. Stress-dependent parameters: *Water Resources Research*, v. 12, no. 3, p. 375–391.
- , 1977, Estimating parameters of compacting fine-grained interbeds within a confined aquifer system by a one-dimensional simulation of field observations, *in* Land subsidence symposium: Proceedings of the second International Symposium on Land Subsidence, held at Anaheim, California, 13–17 December 1976: International Association of Hydrological Sciences, IAHS-AISH Publication series, no. 121, p. 145–156.
- , 1978, Field verification of a one-dimensional mathematical model for transient compaction and expansion of a confined aquifer system, *in* Verification of mathematical and physical models in hydraulic engineering: Proceedings, 26th annual Hydraulics Division specialty conference, University of Maryland, College Park, Maryland, August 9–11, 1978: New York, American Society of Civil Engineers, p. 189–196.
- Ireland, R.L., 1986, Land subsidence in the San Joaquin Valley, California, as of 1983: U.S. Geological Survey Water-Resources Investigations Report 85-4196, 50 p.
- Ireland, R.L., Poland, J.F., and Riley, F.S., 1984, Land subsidence in the San Joaquin Valley, California, as of 1980: U.S. Geological Survey Professional Paper 437-I, 93 p., 1 pl. in pocket.

- Johnson, A.I., 1984, Laboratory tests for properties of sediments in subsiding areas, pt. 1, chap. 4 of Poland, J.F., ed., *Guidebook to studies of land subsidence due to ground-water withdrawal*: Paris, UNESCO, Studies and Reports in Hydrology 40, p 55–88.
- Johnson, A.I., Moston, R.P., and Morris D.A., 1968, Physical and hydrologic properties of water-bearing deposits in subsiding areas in central California: U.S. Geological Survey Professional Paper 497-A, 71 p., 14 pls.
- Jorgensen, D.G., 1980, Relationships between basic soils-engineering equations and basic ground-water flow equations: U.S. Geological Survey Water-Supply Paper 2064, 40 p.
- Lofgren, B.E., 1976, Hydrogeologic effects of subsidence, San Joaquin Valley, California: International Symposium on Land Subsidence, 2nd, Anaheim, Calif., December 13–17, program and abstracts, no. 12, unnumbered pages.
- 1979, Changes in aquifer-system properties with ground-water depletion, in Saxena, S.K., ed., *Evaluation and prediction of subsidence*: New York, American Society of Civil Engineers, p. 26–46.
- Lofgren, B.E., and Klausning, R.L., 1969, Land subsidence due to ground-water withdrawal, Tulare–Wasco area, California: U.S. Geological Survey Professional Paper 437-B, 23 p.
- Lohman, S.W., 1972, Definitions of selected ground water terms—Revisions and conceptual refinements: U.S. Geological Survey Water-Supply Paper 1988, 21 p.
- McClelland, E.J., 1962, Aquifer-test compilation for the San Joaquin Valley, California: U.S. Geological Survey Open-File Report [62-80], 40 p. (rev. 1966).
- Page, R.W., 1986, Geology of the fresh ground-water basin of the Central Valley, California, with texture maps and sections: U.S. Geological Survey Professional Paper 1401-C, 54 p., 5 pls. in pocket.
- Poland, J.F., 1961, The coefficient of storage in a region of major subsidence caused by compaction of an aquifer system, in *Geological Survey Research 1961*: U.S. Geological Survey Professional Paper 424-B, p. B52–B54.
- Poland, J.F., Lofgren, B.E., and Riley, F.S., 1972, Glossary of selected terms useful in studies of the mechanics of aquifer systems and land subsidence due to fluid withdrawal: U.S. Geological Water-Supply Paper 2025, 9 p.
- Poland, J.F., Lofgren, B.E., Ireland, R.L., and Pugh, R.G., 1975, Land subsidence in the San Joaquin Valley, California, as of 1972: U.S. Geological Survey Professional Paper 437-H, 78 p.
- Prudic, D.E., and Williamson, A.K., 1986, Evaluation of a technique for simulating a compacting aquifer system in the Central Valley of California, U.S.A., in Johnson, A.I., Carbognin, Laura, and Ubertini, Lucio, eds., *Land subsidence: Proceedings of the Third International Symposium on Land Subsidence held in Venice, Italy, 19-25 March 1984*: Wallingford, Oxfordshire, IAHS Press, Institute of Hydrology, IAHS publication 151, p. 53–63.
- Riley, F.S., 1969, Analysis of borehole extensometer data from central California, in Tison, L.J., ed., *Land subsidence*: [Brussels], IASH–Unesco, International Association of Scientific Hydrology Publication 89, v. 2, p. 423–431.
- 1998, Mechanics of aquifer systems—The scientific legacy of Joseph F. Poland, in Borchers, J.W., ed., *Land subsidence case studies and current research: Proceedings of the Dr. Joseph F. Poland Symposium on Land Subsidence*: Belmont, Calif., Star Publishing Co., Association of Engineering Geologists Special Publication 8, p. 13–27.
- Riley, F.S., and McClelland, E.J., 1971, Application of the modified theory of leaky aquifers to a compressible multiple-aquifer system: *Mechanics of aquifer systems: Analysis of pumping tests near Pixley, California*: U.S. Geological Survey Open-File Report, 96 p.
- Sneed, Michelle, and Gallaway, D.L., 2000, Aquifer-system compaction and land subsidence: Measurements, analyses, and simulations—the Holly Site, Edwards Air Force Base, Antelope Valley, California: U.S. Geological Survey Water-Resources Investigations Report 00-4015, 65 p.
- Terzaghi, Karl, 1925, *Principles of soil mechanics: IV; settlement and consolidation of clay*: *Erdbaummechanik*, v. 95, no. 3, p. 874–878.
- 1943, *Theoretical soil mechanics*: New York, Wiley, 510 p.
- U.S. Bureau of Reclamation, 1974, *Earth manual: A guide to the use of soils as foundations and as construction materials for hydraulic structures* (2nd ed.): U.S. Department of the Interior, Bureau of Reclamation, Water Resources Technical Publication series, 751 p. [Reprinted 1980].
- Williamson, A.K., Prudic, D.E., and L.A. Swain, 1989, *Ground-water flow in the Central Valley, California*: U.S. Geological Survey Professional Paper 1401-D, 127 p.